MASTERARBEIT

Titel der Masterarbeit

"Combining Raman microspectroscopy and heavy water (D₂O) to identify the active members in microbial communities with single cell resolution"

verfasst von

Esther Mader, BSc

angestrebter akademischer Grad

Master of Science (MSc)

Wien, 2015

Table of content

1. Introduction

1.1 Functional markers for microbial activity

The classical approach to identify and study the physiology and function of organisms in microbiology is based on isolation and culturing followed by nutritional and biochemical tests (e.g. Derrien et al., 2004; Miyamoto and Itoh, 2000). As cultivation is labor as well as time intensive and only a minor fraction of the microbial community grows under laboratory conditions, the development of cultivation independent methods is worthwhile. For this purpose (stable) isotopes are widely used in microbial ecology. They allow tracing the path of specific substrates in a complex environment and in combination with molecular techniques, they also allow to identify active members within a population (Berry et al., 2013; Boschker and Middelburg, 2002; Radajewski et al., 2000; Wagner et al., 2006). This simultaneous identification and characterization of microorganisms within their natural environment makes it possible to see spatial distribution and interaction between different species. Most common are $^{13}C/^{14}C$ labeled substrates (Haider et al., 2010; Li et al., 2013; Sixt et al., 2013) which provide a wide range of possible applications. Other options are the use of ^{15}N (Buckley et al., 2007; Roh et al., 2009), ^{18}O (Aanderud and Lennon, 2011; Ye et al., 2009) or deuterium (^{2}H) (Alexandrino et al., 2001; Ong et al., 2002), but not all desired substrates are readily available or can be purchased at all.

However, these methods are coupled to the addition of an isotopic labeled compound that allows only the investigation of specific functional groups and/or specified processes in the system. It also often alters the concentration and availability of this specific compound hence the community composition possibly changes. To overcome these challenges substrates are desirable that are generally available in all environments and do not influence the substrate concentration. Additionally they should be used equally by all members of the community and therefore serve as an unspecific general activity marker.

1.1.2 Deuterium

Deuterium is a rare isotope with an abundance of about 150ppm (0.015 atom%) in seawater (Somlyai et al., 1993). The ratio of deuterium to hydrogen is 1/6600 which leads – because of the lower ionization constant of D_2O (1.95×10^{-15}) compared to H_2O (1.008×10^{-14}) – to a ratio of deuterons to protons of ~1/15000 (Olgun, 2007). This means that in all biological processes involving protonation there is a 1/15000 chance of deuteronation. After deuterium was first enriched and isolated in the 1930s the possibility of isotopic effects was studied intensively. It was demonstrated that deuterium and hydrogen react at different rates and that the reactivity of bonds to deuterium is generally lower than of the corresponding bonds to hydrogen. As a result, the isotopic effect was then widely used to study mechanisms of chemical reactions

(Wiberg, 1955). Furthermore, a study of De Giovanni (1960) indicated that the isotopic effect of deuterium causes inhibition of bacterial cell growth when used in high concentrations.

Responsible for this relatively strong isotopic effects are presumably three factors:

- the relatively high difference in free energy between the isotopes
- the difference in mass (has an effect on the velocity of passage over the potential-energy barrier and the possibility for non-classical penetration of the energy barrier)
- the D-bond is more stable than the corresponding H-bond (Wiberg, 1955).

Nevertheless, several studies reported that bacteria are able to grow in medium containing D_2O (Butler and Grist, 1984; De Giovanni, 1960; Tulis and Eigelsbach, 1970) and that deuterium from environmental water is incorporated into the bacterial cell mass (De Giovanni and Zamenhof, 1963). Furthermore it was demonstrated that all hydrogen in fatty acids of *Desulfobacterium autotrophicum* derive from water (Campbell et al., 2009) and *Desulfosarcina variabilis* was found to obtain 80% of the lipid hydrogen from water, when grown autotrophically on H_2 (Wegener et al., 2012). Therefore the substitution of hydrogen with deuterium in the growth water will lead to isotopically labeled cell membrane lipids. These findings open the possibility to use D_2O as a general activity marker in environmental studies without altering the substrate availability and thus prohibit possible changes in cell activity and community composition.

1.2 Raman spectroscopy

Raman spectroscopy is a fast and nondestructive method to gain information about the chemical bonds and the molecular composition of a sample (Wagner, 2009). Moreover, it provides a high spatial resolution (in the range of 1 μm), allowing the analysis of single cells (Harz et al., 2009). All components present in a cell contribute to the Raman signal, which therefore reflects their overall molecular composition. In contrast to other spectroscopic methods (e.g. UV/VIS, Infra-Red) this method is based on molecular vibrations induced by the interaction of photons with the molecules. The vibrational spectra of bacterial cells share similar bands, but they also allow taxonomic discrimination as the relative amounts of these compounds vary between species and strains (Harz et al., 2009).

1.2.1 Historical development

The inelastic scattering of light was predicted by A. Smekal in 1923 and was proven only 5 years later by C. V. Raman and K. S. Krishnan. The visual observation of light being scattered by a liquid showed that most of the emerging light has the same color as the incident light. However a small fraction of the light appeared with a different color, which was isolated by placing a filter in between the sample and the observer. This was demonstrated for approximately 60 different liquids. Raman subsequently replaced the

observer with a spectroscope to measure the exact wavelength of the incident and the scattered light obtained (Bohning et al., 1998). He found that the scattered spectrum of each liquid present distinct lines but similarities could be observed in liquids with chemically similar groups (Raman and Krishnan, 1928). In 1930 Raman received the Nobel Prize in Physics for his work.

One problem of Raman spectroscopy in its beginnings was the lack of a light source with a sufficient high intensity and the very low signal intensity that is obtained (Bohning et al., 1998). The development of monochromatic lasers, which provide a high intensity, single frequency beam was an important step for the development of modern Raman technology. With the implementation of this light source a huge increase in signal to noise ratio was obtained. The second important improvement was the implementation of cooled Charge-Coupled-Device (CCD) detectors, as these can provide the high sensitivity and resolution necessary for Raman spectroscopy of microbial cells. Today a wide range of laser wavelengths (near UV to near IR) are used to optimize for specific sample requirements (Harz et al., 2009; Petry et al., 2003).

1.2.2 Function

Spectra in Raman spectroscopy do not originate from absorption or emission of light like other spectroscopic methods, but rather derive information from inelastic light scattering ("Raman effect"). The Raman effect depends on the atomic bonds and vibrations within a molecule leading to a characteristic molecular vibration, and therefore enables identification of the structure and composition of a substance even in mixed samples, by observation of the resulting spectrum.

When a photon hits a molecule it interacts with the electrons and these electrons are excited to a virtual state in which they possess a higher energy level. When the electron falls back to its ground state the energy is released and scattered photons with the same frequency and wavelength as before are observed (Rayleigh scattering) (Fig. 1B). In some rare cases the electron does not return to its natural ground state but instead settle on a vibrational state (slightly higher energy potential than ground state) this results in a released photon with a lower wavelength than the incident photon (Raman Stokes scattering) (Fig. 1C). Another possibility is that the electron, interacting with the incident photon, is already on a vibrational state and returns to its ground state after excitation. This leads to a released photon with a higher frequency, in a process called Anti-Stokes Raman scattering (Fig. 1D). Rayleigh scattering is an elastic scattering process and is 10^8 times more likely than the inelastic Raman scattering (Petry et al., 2003).
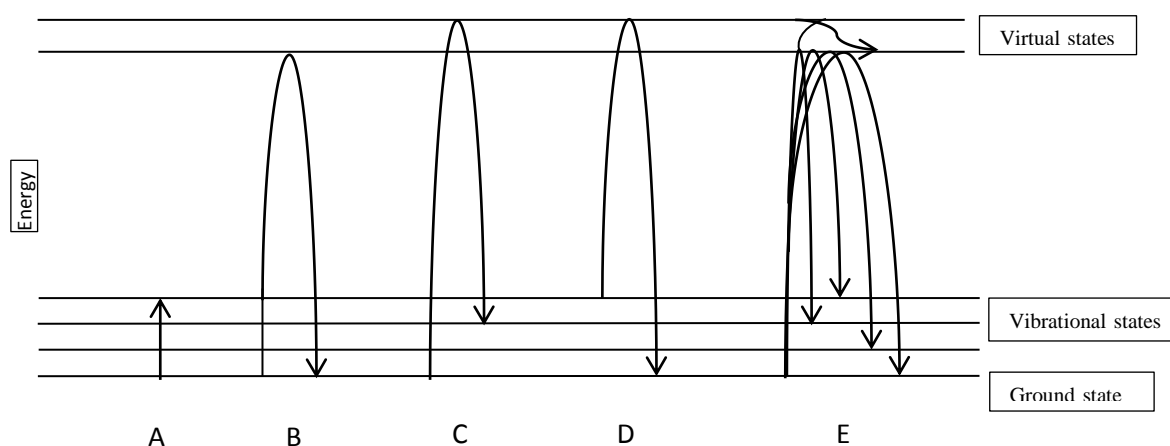
Figure 1: Schematic illustration of the different energy states conducted during spectroscopic analysis. (A) IR absorption, (B) Rayleigh (elastic) scattering, (C) Raman Stokes (inelastic) scattering, (D) Raman Anti-Stokes (inelastic) scattering and (E) fluorescence.

In the Raman spectrometer the dominant Rayleigh scatter is filtered out to detect the Raman Stokes scattered photons, which are plotted depicting the energy difference between the incident and scattered photons. The resultant spectra show narrow peaks which are unique for molecular bonds and therefore provide a fingerprint of the molecular structure of the sample.

1.2.3 Raman spectroscopy and stable isotope probing

The incorporation of heavy isotopes into a molecule leads to a shift of the respective Raman bands (Huang et al., 2004). Therefore the incorporation of these isotopes, in the course of a stable isotope labeling study, can be detected. This was proven for ^{13}C labeled glucose which lead to red shifted (peak shift toward shorter wave numbers) protein and nucleic acid signals in seven different bacterial species (Huang et al., 2004) as well as for ^{13}C labeled phenylalanine in chlamydial cells which resulted in a red shift of the phenylalanine denoted peak (Haider et al., 2010). The shift of isotopically labeled Raman bands is exemplarily depicted in Figure 2 on the example of ^{13}C fed *E. coli* cells.
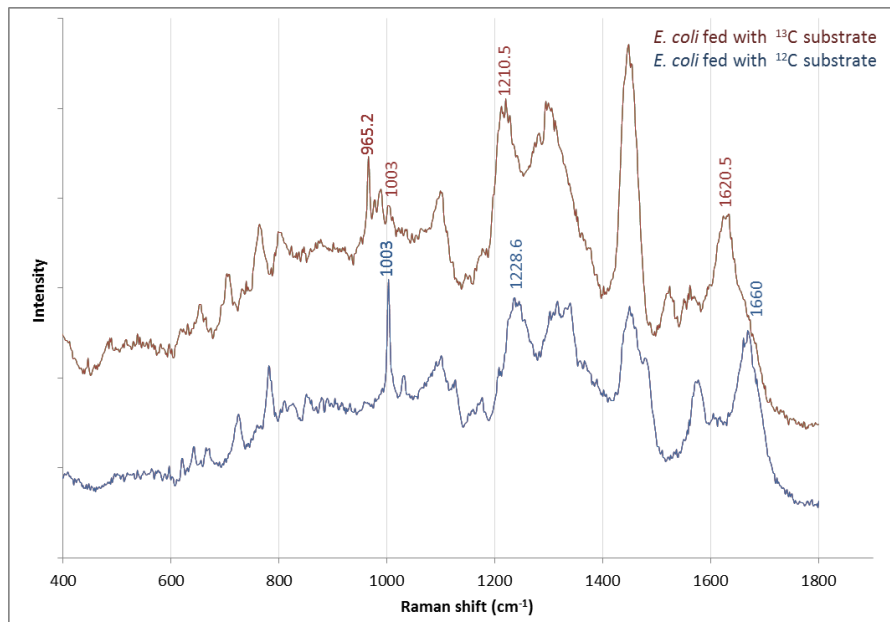
Figure 2: Example of ^{13}C induced peak shift in *Escherichia coli* Raman spectra. The red shift of phenylalanine (1003 cm^{-1}) is used as signature peak. *E. coli* were fed with 100% ^{13}C containing substrate leading, in the upper red spectra to a clear shift of the phenylalanine peak situated at 1003 cm^{-1} to 965 cm^{-1}. Additional shifts of the protein denoted peaks (1228 cm^{-1} and 1660 cm^{-1} to 1210 cm^{-1} and 1620 cm^{-1}) are visible. Spectra recorded by Christoph Böhm.

Similar to ^{13}C, it was demonstrated that the exchange of ^{1}H with ^{2}H causes a red shift in the spectra of HeLa cells (van Manen et al., 2008). This shift is more pronounced as the mass difference between the heavy isotope deuterium to hydrogen is larger than between the carbon isotopes. The minimum concentration for a reproducible spectral shift with ^{13}C labeled microbial cells was determined to be 10 atom% (Huang et al., 2007). The usability of heavy water as a general activity marker in microbial populations will depend on the strength of the peak shift in correlation to the isotopic effect of deuterium.

To test this approach, different bacterial strains grown in increasing concentrations of D_2O were tested and the assimilation of the heavy isotope and the growth rate of the microbes were observed. Based on these data the percentage of D_2O necessary to obtain reasonable signals with Raman microspectroscopy and the cultivation time needed to label cells sufficiently, without inhibiting growth was estimated. Furthermore it was tested if different organisms show similar rates of inhibition and assimilation. The implementation of D_2O to effectively detect active bacterial cells with Raman microspectroscopy was found to be a promising tool for the application in more complex environments as well. The possible combination of Raman based stable isotope probing with fluorescence in situ hybridization (FISH) as shown by Huang et al. (2007) allows to study the function and physiology of non-cultured cells. By combining this method with D_2O as a general activity marker, the activity rates in the entire community can be compared to the activity of selected species.

To explore this application the method was tested on a mouse cecum community. The D_2O concentration was set relatively high so that a good and visible signal could be anticipated but not as high that an interference of bacterial cell growth would be expected.

1.3 Environmental sample

As mentioned in the beginning, only a small fraction of microorganisms are cultivable in the lab, therefore the assumptions of physiology and function of new, not yet cultivated, species is mostly based on genomic and metagenomic data. Based on the genes of a microorganism one can hypothesize the metabolism and therefore the function of these microbes in their ecosystems (Gill et al., 2006; Haferkamp et al., 2006; Qin et al., 2010). The development of high throughput sequencing techniques enabled studies that explore the phylogenetic diversity of highly complex microbial communities. This has revealed an unexpected amount of species that are only present in a very low abundance (Galand et al., 2009; Sogin et al., 2006) but some of these rare genera were found to perform important functions within the system despite their low cell count (Montoya et al., 2004; Pester et al., 2010).

A recognized problem of these techniques is that, the genomic potential of an organism does not demonstrate its function or activity. Furthermore a substantial fraction of the genomic data acquired is not well-represented by reference genomes or belong to novel species and therefore their function cannot be denoted reliable (Dave et al., 2012; Qin et al., 2010; Tap et al., 2009). This leads to a limited understanding of the functional potential of the microbes in complex environments, for instance the gut (Qin et al., 2010). Stable isotopes on the other side show metabolic pathways and functions directly in the environment (Huang et al., 2009).

1.3.1 The gut community

The colon harbors the highest cell density in the intestinal tract with estimated 10^{11} cells per milliliter (Doré and Corthier, 2010; Walter and Ley, 2011). The vast majority of cells found in the gut community are bacteria (eukaryotes: 0.5%, archaea: 0.8%, viruses up to 5.8%) (Dave et al., 2012). It has been estimated that up to 40,000 species reside in the gut ecosystem (Tap et al., 2009). From this only a few dominant phyla were found which are present in a high abundance and are found in all hosts, within these phyla the species richness is very high and differs strongly from individual to individual. The dominant and most abundant microbiota belong to the phyla *Firmicutes* and *Bacteroidetes* (Eckburg et al., 2005; Tap et al., 2009; Turroni et al., 2008; Walter and Ley, 2011).

Studies revealed that, like in other ecosystems a substantial proportion of gut microbiota match ribosomal sequences from uncultured bacteria. Up to 80% of species in the gut community are estimated to be not yet cultivable because of their complex dependence on one another and their fastidious anaerobic and nutrients requirements

(Dave et al., 2012). This supports the assumption that the identity and thus functional importance of some community members might have been overlooked so far.

1.3.2 Function

The gut microbiota fulfills a variety of functions in the host organism. They contribute essentially to the maturation of the host immune system (Dave et al., 2012) and serve as barrier against colonization by pathogens by competing with them for nutrients and ecological niches (Dave et al., 2012; Doré and Corthier, 2010). Besides, they are vital to the breakdown of complex carbohydrates to simple monosaccharides. Compared to the human genome, the gut microbiome has more genes involved in starch and sucrose metabolism (Gill et al., 2006) by which the conversion of complex sugars to short chain fatty acids is facilitated, so these can be absorbed by the host as energy source (Qin et al., 2010). Additionally they are involved in the production of a variety of essential vitamins like biotin, riboflavin, pantothenate, folate, ascorbate, (Arumugam et al., 2011) and cobalamine (B_{12}) (Albert et al., 1980). The mucus layer covering the intestinal tract acts as a barrier for the microbiota and supports bacterial growth by providing nutrients like saccharides (Turroni et al., 2008). The main functions of the microbiome were found to be redundant among species which indicates a great robustness of the system (Dave et al., 2012).

1.3.3 Species for strain specific activity survey

As mentioned above, the phylum *Bacteroidetes* is one of the biggest groups present in the intestinal tract, and therefore the functionality of species in this phylum is of great interest for the understanding of the complex community. The genus *Bacteroides*, belonging to the phylum *Bacteroidetes,* was identified before as the most abundant but also the most variable genus in the microbiome (Arumugam et al., 2011). These strains are highly heterogeneous both physiological and biochemically as well as in terms of cellular morphologies (Weiss and Rettger, 1937). Nevertheless, based on dominant functional genes found in the *Bacteroides* strains they derive energy primarily from carbohydrates and proteins through fermentation (Dave et al., 2012).

1.3.3.1 Bacteroides acidifaciens

The strain *B. acidifaciens* was specifically targeted in this study as it was identified as a dominant host compound degrader in the gut (Berry et al., 2013). The cells are gram negative rods and obligate anaerobs. Grown on EG agar plates they reach a size of 0.8-1.3 x 1.6-8.0 µm. The name acidifaciens corresponds to the ability to lower the pH of peptone-yeast broth, which was used as growth medium to isolate the strains. The isolates are divided into two groups by 16S rRNA sequence homology (Miyamoto and Itoh, 2000).

1.3.3.2 Akkermansia muciniphila

The degradation of mucus in the gut is an important regulatory mechanism therefore the organisms performing this task are of interest for all studies concerning the basic

ecological niches in this environment. *Akkermansia muciniphila* is a member of the division Verrucomicrobia, which was found to be a dominant mucin degrader in the gut. Verrucomicrobia constitute only about 0.1% (Tap et al., 2009) to 1% (Muyzer et al., 1993) of the gut microbiota in contrast to *Bacteroidetes* which were calculated to contribute 16.9% (Tap et al., 2009) of the overall community members. It was supposed that *Akkermansia* is the predominant degrader of the mucus layer in the gut, as *A. muciniphila* was found to be the fastest growing mucin degrading organism in the gut community. It grows on gastric mucin without the addition of vitamins or other substrates to a higher cell density than other strains isolated from the microbiome (Derrien et al., 2004). Mucin is used as sole carbon, energy and nitrogen source, for this obligate chemo-organotroph and strictly anaerobic gram negative organism (Muyzer et al., 1993). *Akkermansia* are oval shaped with a size of ~0.6-1 µm along the long axis and grow as single cells or pairs and often forms aggregates. Optimal growth is reached at 37°C (growth occurs between 20-40°C) with a doubling time of approximately 1.5 h (Derrien et al., 2004).

The aim of this study was to establish a protocol to successfully detect deuterium assimilation in microbial cells derived from D_2O in the growth medium by Raman microspectroscopy. The successful application of this new method of stable isotope probing encourages exploring further fields of possible applications in other environments and evaluating its benefits and possible drawbacks in ecological studies.

2. Materials and methods

2.1 Growth of pure cultures on media containing deuterated water

2.1.1 Bacterial strains
Three fast growing heterotrophic bacterial strains, *Escherichia coli* DH10B, *Bacillus subtilis* W23 and *Bacillus thuringiensis* ATCC 10792 were grown in rich media at 37°C, shaking at 150 rpm overnight to stationary phase.

For the experiments 5 ml D_2O containing medium was inoculated with 50 µl of stationary phase culture and incubated at 37°C on an orbital platform shaker (150 rpm, innova 2300, New Brunswick scientific, Enfield, USA) in triplicates. Therefore Lysogeny-Broth (LB) medium, containing 1 g peptone, 0.5 g yeast extract, 0.5 g NaCl filled up to 100 ml with H_2O (MQ – Mili-Q® water purification system) or D_2O (Sigma, 99.9% isotopic purity) was prepared. To prevent changes in D_2O concentration by autoclaving (De Giovanni and Zamenhof, 1963) it was filter sterilized (0.2 µm syringe filter, Thermo scientific). To obtain medium with concentrations of 0, 2.5, 5, 10, 15, 20, 30, 50 and 100% D_2O the media containing either H_2O or D_2O were mixed by volume. Regularly (every 30 min) the OD_{578} nm was measured. When the cultures reached an OD of about 0.6 a 1:7 diluted aliquot was used to ensure accurate measurements. The cultures were harvested after reaching stationary phase (OD=0.8-0.9), PFA fixed and stored in a 1:1 EtOH/phosphorous buffer solution (PBS) at -20°C until further investigation.

2.1.2 Cell fixation (PFA fixation)
For cell fixation 1 ml of stationary phase culture was centrifuged at 20 817 g for 5 min, the supernatant was discarded and the sample was washes with 1x PBS followed by a second centrifugation for 5 min at 20 817 g. Subsequent 4% PFA in PBS (3:1) was added and the sample was incubate at 4°C for 3 h centrifuged for 5 min at 20 817 g and washed with 1x PBS. For storage at -20°C the sample was suspended in a mixture of equal amounts of 1x PBS and 96% EtOH.

2.1.3 Growth curves
Optical density is considered to be proportional to bacterial density (Monod, 1949) and therefore allows to calculate the doubling time of microbial cultures indirect. OD values were used to display growth curves of the incubations containing different amounts of deuterium using Microsoft Excel 2010. Further the doubling time was calculated to assess the influence of high concentrations of deuterated water in the growth medium.

2.2 Raman spectroscopy
The PFA-fixed samples of the pure cultures were thoroughly vortexed and about 0.5-1 µl (depending on the density of the culture) were pipetted onto an aluminum coated carrier slide (Al136, EMF Corporation). Subsequently dried for 5-10 min at 46°C and dipped into double distilled water (MQ) for a few seconds to remove salts. The excess

water was dried with compressed air. The dried sample can be stored at RT for several days.

The Raman spectra were obtained using a confocal Raman spectrometer (Horiba, HR800 or Evolution) combined with a light microscope (Olympus, BX41) and an x100 Mplan-achromate objective (Olympus) with a numerical aperture of 0.09. The Raman scattering was achieved by an Nd:YAG laser at a wavelength of 532.09 nm. Every day before measurement the spectrometer was calibrated on pure silica using the calibration script included in the LabSpec5 software.

To acquire a spectrum of the fingerprint region (400-1800 cm^{-1}) as well as the CH peak (around 2900 cm^{-1}), which is assigned to cell wall lipids mainly, an acquisition range from 400 to 3200 cm^{-1} was used. A 600 line/mm grating (Horiba Evolution 600 line/mm) was used which required an extended range measurement to achieve the desired spectral width. For this purpose the cells were measured twice and the two separate spectra were automatically combined within the Labspec5 software. Because the aluminum coated slides reflect the laser light and therefore heighten the spectra intensity, a gray filter (D1) which allows approximately 8% laser intensity (Böhm, 2012) was used to get a good peak-background ratio. Measuring time was set between 30 and 120 sec. To reduce the background noise of the spectra in some cases a shorter measuring time with multiple intervals was chosen, this multiple measurements were than processed within the LabSpec5 software to form an accumulated spectrum. As the intensity between the two spectra can differ, an automatic intensity adjustment within Labspec5 was conducted. For statistical analysis 20-30 single cell spectra of each sample were acquired.

2.2.1 Process raw data

The spectral data were mean normalized by dividing every data point (of a wavenumber) by the sum of all data points of each spectrum. Furthermore, the intensity was leveled to "Zero" by setting the lowest intensity pixel of each spectrum to zero using the LabSpec5 software implemented in the instrument. The spectra were than manually aligned to the phenylalanine peak (Phe 1003 cm^{-1}). In addition average spectra of each pure culture were calculated and visualized using Microsoft Excel 2010.

In addition, the raw data were normalized and baselined using the R software (R Development Core Team. 2011). The incorporation of D was estimated based on the CD (2.040-2.300 cm^{-1}) and CH (2.800-3.100 cm^{-1}) peak area. For this purpose the peak area ratio (%CD) was calculate by CD/(CD+CH). The %CD was displayed and the linear regression was calculated. Also, the detection limit (mean plus 3x s.d. of the measurements of cells grown without deuterium) was displayed to determine the minimum D_2O concentration necessary to ensure a reliable label.

2.3 NanoSIMS

For optimal measurements with NanoSIMS it is essential to obtain an even distribution of sample material. Fixed *E. coli* cells grown with 0, 15, 30, 50 or 100% D_2O in the growth medium as well as *Bacillus subtilis*, *Bacillus thuringiensis* and *Methanobrevibacter smithii* grown with 30% D_2O were pipetted in a single layer of separated cells onto boron-doped silicon wafers (7 x 7 x 0.7 mm; Active Business Company GmbH, Munich, Germany). The cells were air dried at RT and washed carefully with double distilled (MQ) and additionally sterile filtered H_2O. NanoSIMS measurements were carried out on a NanoSIMS NS50L instrument (Cameca, Genevilliers, France). Data were simultaneous acquired for $^{12}C^1H^-$, $^{12}C^2H^-$, $^{16}O^1H^-$, $^{16}O^2H^-$, $^{12}C^{14}N^-$, $^{31}P^-$ and $^{32}S^-$ secondary ions. $^{16}OH^-$ and $^{12}CH^-$ molecular ions were selected for determination of the hydrogen isotope composition. Instrumental measurements were carried out by Arno Schintlmeister, for detailed information see Berry et al., 2015. For the *Bacillus* strains additionally Raman measurements were conducted.

The obtained secondary ion intensities were corrected for the contribution of ^{13}C and ^{17}O natural carbon and oxygen isotope abundances (isotopic ratios of $^{13}C/^{12}C$ and $^{17}O/^{16}O$) which are on average 0.0109 and 0.000380 (de Laeter et al., 2009). This approach was evaluated by measurements on *E. coli* cells grown without addition of D_2O.

Images from the center of the cells were chosen for data analysis using the WinImage Software package (Cameca). The image layers were aligned to compensate positional shifts occurring during long acquisition times. In the following the image stacks were accumulated and the secondary ion signal intensity was dead time corrected on a per pixel basis. The regions of interest (ROIs) were manually defined referring to individual cells, based on the $^{12}C^{14}N^-$ and $^{31}P^-$ secondary ion images. The morphology of the selected ROIs was confirmed in the secondary electron intensity distribution images. Hydrogen isotope composition images were generated based on the D/(H+D) isotope fraction values for each individual pixel, which were inferred from the recorded $^{12}CH^-$ and $^{16}OH^-$ secondary ion signal intensity by

$$\frac{D}{(H+D)} = \frac{^{12}C^2H^-_{corr}}{\left(^{12}C^1H^- + {}^{12}C^2H^-_{corr}\right)} \text{ and } \frac{D}{(H+D)} = \frac{^{16}O^2H^-_{corr}}{\left(^{16}O^1H^- + {}^{16}O^2H^-_{corr}\right)}.$$

The subscript *"corr"* at the signal intensities of the deuterium containing secondary ion species refers to the subtraction of the isobaric $^{13}C^1H^-$ and $^{17}O^1H^-$ ions, respectively which are detected simultaneous. It has to be stated that this correction leads to a bias if the actual ^{13}C content of the sample is unknown.

For different samples the secondary ions (OH$^-$, CH$^-$) which obtained a higher yield were chosen. These were for *M. smithii* cells, OH$^-$ ions whereas CH$^-$ ions were the species of

choice for *E. coli*.

2.4 Environmental sample

2.4.1 Incubation of mouse cecal content

To test the applicability for ecological studies the deuterium incubation was tested in a complex environmental sample. Therefore three adult mice C57BL/6 were sacrificed and the cecum contents were extracted in an anaerobic tent. The cecal content was homogenized with PBS containing 50% D_2O by vortexing and divided into small glass vials. The samples were amended with 3.33 mg/ml glucose, 3.33 mg/ml glucosamine, 3.33 mg/ml mannose or 1% mucin (porcin gastric mucin, Sigma). As control one sample of each mouse was left without amendment. The vials were closed and incubated anaerobically at 37 °C overnight. Following 1 ml of the cecal incubation was PFA fixed and stored at -20°C until further investigation.

2.4.2 Fluorescence in situ Hybridization (FISH)

The PFA fixed samples were diluted to the desired density (1:100 for conventional or 1:10 for Raman FISH) in a mixture of equal amounts of PBS and 96% EtOH. To determine which populations to choose for the Raman FISH approach, first conventional FISH following the protocol of (Daims et al., 2004) was performed to detect species with a sufficient abundance in the samples. For this purpose 10 µl of PFA fixed sample were used per well. Hybridizations were conducted for 3 h using various indocarbocyanine (Cy3) or indodicarbocyanine (Cy5) labeled, strain specific probes always combined with a fluorescine (Fluos) labeled general bacterial probe.

2.4.3 Quantification (daime)

For quantification of the cecum incubations 20 randomly chosen areas from each FISHed sample were recorded with a confocal laser scanning microscope (Leica TCS SP8 X). The quantification of the selected species was done with daime 2.0 (Daims et al., 2006). Therefore, the separated colors channels were segmented and objects were automatically selected within the software. Signals resulting from background fluorescence were rejected manually. To determine the abundance of the specific strains the volume fraction of the strain specific signals were correlated to the general population probe. The "total biovolume fraction" was utilized to compare the abundance of the examined strains in the different incubations.

2.4.4 Fluorescnece in situ hybridization in liquid phase

The samples were gently sonicated (5 sec, 2 cycles) (Sonoplus HD 2070, UW2070; Bandelin, Berlin, Germany) before FISH to detach clustered cells and allow single cell measurements of the identified cells.

For hybridization 10 µl of the respective sample were dehydrated by addition of 50 µl 96% EtOH at room temperature for 5 min and subsequently centrifuged at 20 817 g for 5 min. The supernatant was discarded and the sample was thoroughly resuspended in 10

μl of Hybridization buffer. 1 μl of the respective probe was gently mixed in and the hybridization was carried out at 46°C for 2-3 h, followed by centrifugation at 40°C for 5 min and 20 817 g. The supernatant was discarded and the sample was resuspended in 50 μl pre-warmed washing buffer and incubated for 10 min at 48°C. Samples were collected by centrifugation, resuspended in ice cold 1x PBS/EtOH (1:1) (amount dependent on cell density) and stored at -20°C until measurement.

2.4.4.1 Variations

To examine if the storage conditions or the FISH procedure had an effect on the deuterium content of the cells a series of tests was conducted comparing the spectra of cells treated differently before Raman measurements. To test for the influence of storage conditions no ethanol was added after cell fixation and compared with cells that were undergone the standard procedure. Further *E. coli* cells were measured before and after hybridization and the deuterium peak intensity was compared. To evaluate which factor causes the washout of deuterium, the following variations of the FISH protocol were tested.

- No dehydration before FISH
- No SDS in the hybridization buffer
- No dehydration and no SDS in the hybridization buffer
- Hybridization without formamide
- Hybridization at room temperature
- Hybridization without formamide at room temperature
- Incubation solely in PBS

3. Results

Preliminary tests with *Escherichia coli* grown with either 50% or 100% D_2O in the growth medium revealed a distinct Raman shift related to D_2O assimilation (data from Christoph Böhm, not shown). The wavenumbers of the shifted peak situated between 2040-2300 cm^{-1} were consistent with previous studies on diverse deuterated substances (Falk, 1990; Trumpy, 1935; Walrafen, 1973). It was further demonstrated that adaptation of cells by re-inoculation for several generations is not necessary to reach full label intensity (data from Christoph Böhm, not shown).

Based on the results of the preliminary tests the primary questions for this study were: In what extent does the addition of D_2O influence the growth of microbial cultures and at which concentration does a recognizable shift in the Raman spectrum become visible.

For this purpose 5 different species were grown in the presence of D_2O, partly or completely substituting water in their growth medium.

3.1 Determination of the influence of D_2O on Raman shifts and growth of microbiota

3.1.1 Raman microspectroscopy of deuterated microbial cells

Multiple single-cell Raman spectra of selected species (*Escherichia coli*, *Bacillus subtilis*, *Bacillus thuringiensis*, *Methanobrevibacter smithii*, and *Methanocorpusculum labreanum*) were acquired to determine the deuterium assimilation. The spectra were recorded as described in Materials and Methods with an extended range (400 to 3200 cm^{-1}) to plot the deuterium induced red shift of the CH peak as well as the fingerprint region of microbial cells. Consistent with the preliminary tests a red shift of the CH peak from around 2900 cm^{-1} to about 2200 cm^{-1} was observed in all tested strains. Furthermore the appearance and intensity of the deuterium induced peak was not influenced by repeated measurements of the same cell (10 measurements/cell) confirming the reproducibility of the effect (Fig. S3).

The Raman spectra of all selected strains (20-30 single cells for each species and D_2O concentration) have shown a distinctive CD bond assigned peak. Correlated to increasing D_2O concentrations, the shifted Raman band gained intensity (Fig. 3A). A direct comparison of the Raman spectra of the tested species displayed in Figure 3A revealed a flat area between 1800 and 2600 cm^{-1} in the control incubation grown without D_2O. For the bacterial species a wide range of different D_2O concentrations was tested and is depicted in Figure S1 showing that already at 15% D_2O a small peak shift can be observed. It has to be considered that the CD band was not equally pronounced in all the selected species. The detection limit (mean plus 3x s.d. based on %CD from cells grown without D_2O) was below 1 for all bacterial strains but higher in the archaeal test strains (Fig. S2), which were marked by higher noise due to small cell size and higher autofluorescence.

While the intensity of the shifted peak in *E. coli* and *Bacillus* cells was relatively similar, the CD band of *M. smithii*, and *M. labreanum* had a considerable higher intensity at the same D_2O concentration in the medium. The archaeal strains were only grown with 30% D_2O in the growth medium, therefore the increase in label intensity compared to the bacterial strains associated with higher amounts of deuterium in the growth medium can not be determined.
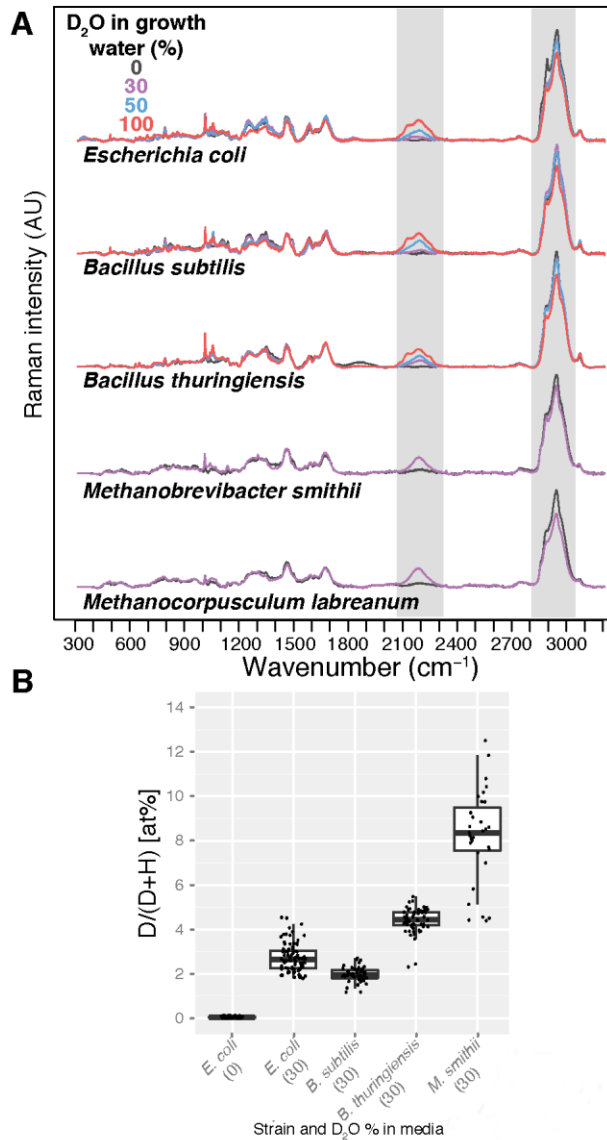
Figure 3: The CD peak in Raman spectra consistently appears in diverse microbial strains. (A) Raman spectra of microorganisms grown in media containing various concentrations of D_2O (grey shaded: CD and CH band). Both methanogens were only grown and tested at a concentration of 30% D_2O in the growth water. **(B)** Comparison of D assimilation in different microbial species grown in 30% D_2O (and *E. coli* without D_2O) as measured with NanoSIMS. Each point represents a single cell spectrum and boxplots represent population quartiles. Graph taken with modifications from Berry et al. 2015.

3.1.2 Deuterium assimilation into cells determined by NanoSIMS

To determine the amount of D assimilation into the cell material during growth NanoSIMS measurements were conducted. For this purpose representative species

16

grown in the presence of 30% D_2O were analyzed. The D isotopic fraction was ascertained and correlated to *E. coli* cells grown without D_2O which were used as a standard for the natural distribution of D in microbial cells. The abundance of D (calculated as described in Materials and Methods) in cells grown without D_2O fluctuated around almost 0 at% (mean 0.02 at%). Therefore no correction in regard of natural occurring D was performed for the following analysis of the deuterium assimilation rate into cell material. Phosphorus was chosen as a representative of cellular biomass and used to confirm the identity of the selected regions as cells.

NanoSIMS measurements of *E. coli* samples grown with different concentrations of D_2O showed an increase in D in the cells correlating with the increase of D_2O concentration in the medium (Fig. 4C+D). This also correlated with an increased CD peak intensity associated with increasing D_2O concentrations (Fig. 4A). Furthermore a decrease of the CH peak intensity correlating to the increase of the CD peak was observed when the difference between the mean spectra of *E. coli* was examined (Fig. 4A+B). In addition a pronounced heterogeneity of D assimilation within one sample was observed by NanoSIMS and became more distinct with increasing concentrations of deuterium in the medium. The variance of incorporated D fluctuated between 8.56 and 25.17 at% D in cells grown with 100% D_2O and 0.78 to 1.45 at% D at a concentration of 15% D_2O in the growth medium (Fig. 4C). The detection limit (mean + 3 s.d. of unlabeled cells) based on the effective assimilation of D in the cell material as determined by NanoSIMS was found to be as low as 0.17 at% D (Fig. 4D).

Additional measurements of two *Bacillus* strains and an autotrophic archaea grown with 30% D_2O substituting the growth water demonstrated differences in the rate of deuterium assimilation in different strains (mean at% D: *E. coli* 2.74, *B. subtilis* 1.98, *B. thuringiensis* 4.42, and *M. smithii* 8.19) (Fig. 3B). In contrast to the bacterial cell cultures the *M. smithii* culture was dominated by extra cellular substances, which were found to be enriched in deuterium and therefore were excluded from the analysis. Nevertheless the archaeal autotroph assimilated substantially more deuterium than the corresponding heterotrophic bacterial test strains which is congruent with the observed differences in the intensity of the deuterium induced peak in the Raman spectra. The incorporation of deuterium into the cellular mass was not uniform for different strains (Fig. 3B) and also varied within the population (Fig. 4D). A direct comparison of the isotopic distribution of D (NanoSIMS) and the corresponding Raman single cell spectrum on the basis of *B. thuringiensis* clearly shows the connection between at% D and %CD for single bacterial cells (Fig. S5).
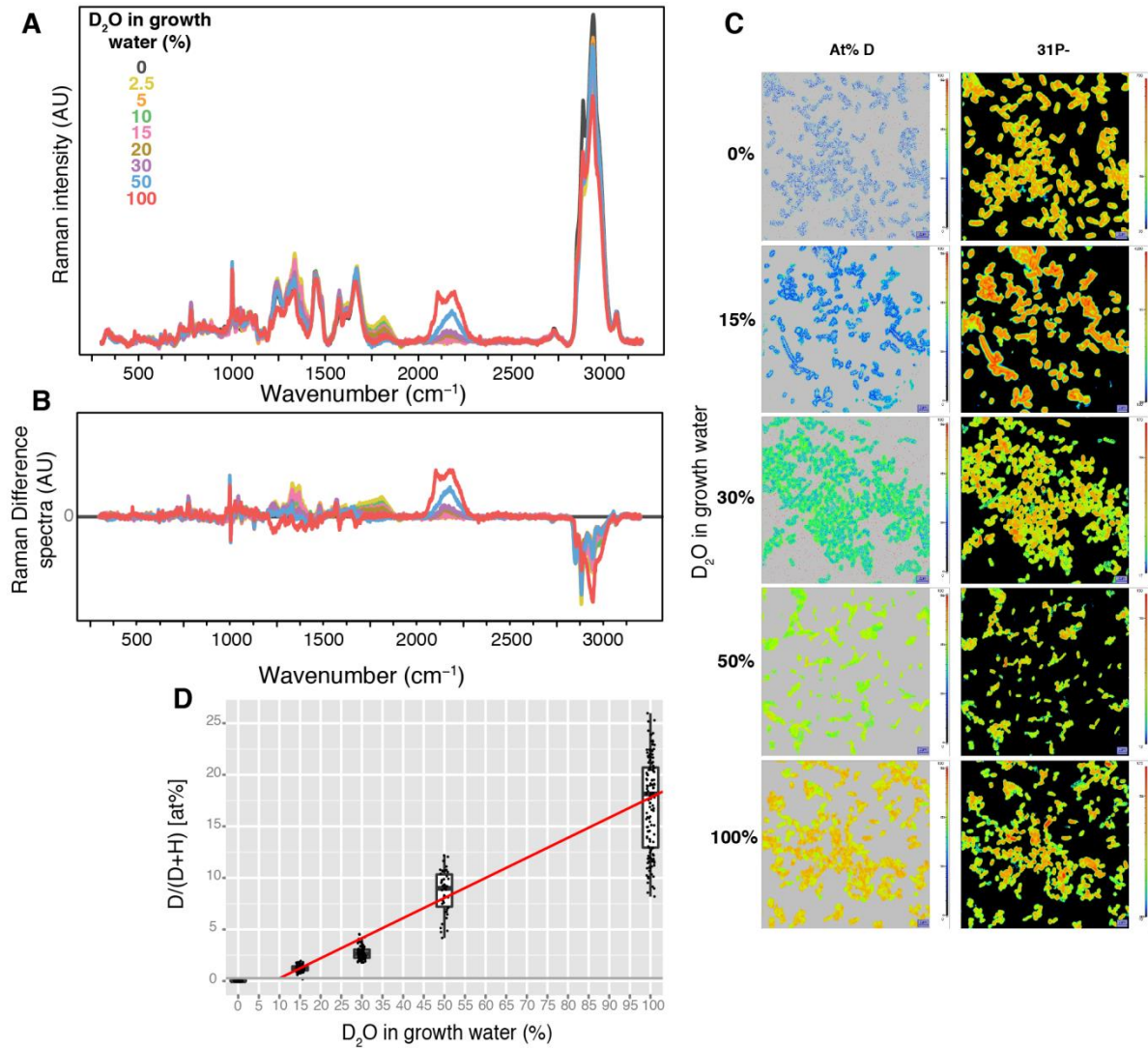
Figure 4: Incorporation of deuterium from heavy water into _Escherichia coli_, detected by Raman microspectroscopy and NanoSIMS. (A) Raman spectra of _E. coli_ grown to stationary phase in media containing heavy water (0, 2.5, 5, 10, 15, 20, 30, 50, and 100 % D_2O). Mean spectra were produced from 10-21 single cell spectra. AU, arbitrary unit. (B) Difference between _E. coli_ Raman spectra (mean). Cells were grown in different concentrations of D_2O or without D_2O. Colors according to part A. (C) D isotope distribution given as atom percent (at%) of _E. coli_ cells from the same experiment detected by NanoSIMS. All images are on the same scale (0-100%). Cellular biomass is indicated by isotopic distribution of $^{31}P^-$. (D) D isotopic fraction determined by NanoSIMS compared to growth water D content. Black dots represent single cells and boxplots show the quartiles for each population. The detection limit (mean plus 3 s.d. of unlabeled cells) is shown in grey (0.17 at% D). D_2O concentration and cellular D content follows a linear regression shown in red (R^2=0.84). Graph adapted from Berry et al., 2015.

3.1.2 The influence of heavy water on the growth of bacteria

The effect of deuterium oxide on the growth rates of three bacterial strains was tested thoroughly. To determine to what extent deuterium affects the growth of bacterial cells the cells were grown with different concentrations of D_2O partly or fully substituting the growth water in LB medium. The optical density (OD$_{578}$ nm) was measured regularly to calculate growth curves (Fig. 5).
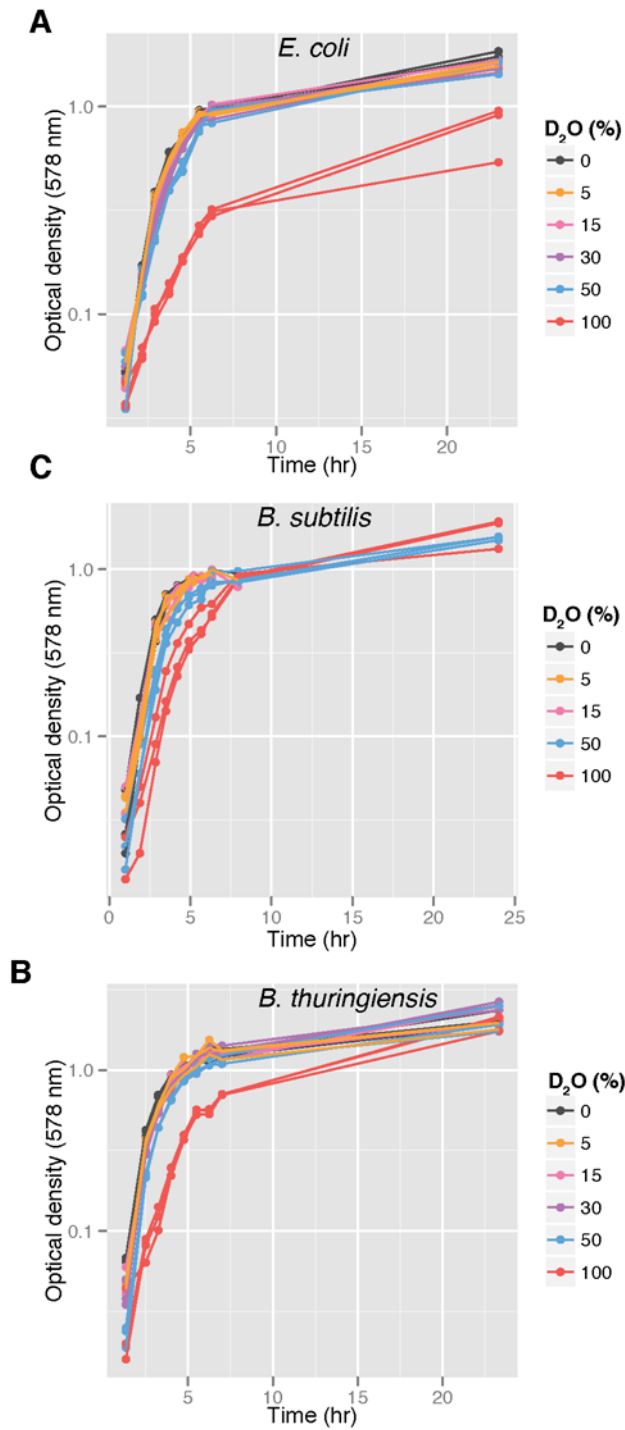
Figure 5: Growth curves of bacteria in the presence of different concentrations of D₂O. Growth curves were obtained from optical density measurements of cultures of (A) *Escherichia coli*, **(B)** *Bacillus thuringiensis*, **and (C)** *Bacillus subtilis*. **The log-phase specific growth rates of** *E. coli* **as well as** *B. thuringiensis* **were decreased in the presence of 100% D₂O (p<0.05) compared to all other concentrations. No significant inhibition of growth was observed for** *B. subtilis* **(p=0.13). Graph taken from Berry et al., 2015 with modifications.**

The growth curves of *Escherichia coli* cultivated in LB medium containing between 0% and 50% D_2O were nearly identical. When the doubling time was calculated only a slight increase with increasing deuterium concentration could be observed with about 36 min at 0% D_2O to 47 min at 50% D_2O. Therefore until the growth water contained 50% D_2O

the increase in doubling time is neglectable, but in medium containing 100% D_2O the logarithmic growth phase becomes flatter and the doubling time increases to around 1.5 h. The growth rates were reduced and the stationary phase does not reach the same optical density as in lower concentrated medium (Fig. 5A).

Similar to *E. coli* also *B. subtilis* shows no differences in growth rates at low concentrations of D_2O in the culture medium (Fig. 5B). The calculated generation times detect only minor differences, it fluctuates between 27 and 33 min. In contrast to *E. coli* when *B. subtilis* was incubated with 100% D_2O a prolonged lag-phase could be observed, but the doubling time was not significantly extended compared to lower concentrations of D_2O, and the same optical density was reached in all cultures.

Concurrent to the species discussed before, no differences in growth rates could be observed for *B. thuringiensis* cultures at low concentrations of D_2O (Fig. 5C). The generation time settles at ~25 min in all cultures from 0% to 50% D_2O. As for the other strains there is no significant deuterium-induced inhibition, visible until all water in the medium is exchanged with D_2O. In cultures containing 100% D_2O the doubling time increased to about 45 min (Fig. 5C).

The growth curves in regard to increasing concentrations of D_2O displayed in Figure 5 indicated that the inhibitory effect of deuterium is not equally pronounced in different strains. In summary it can be stated that at high concentrations of deuterium a prolonged lag phase could be observed, followed by a slower logarithmic phase, but no noteworthy inhibition could be observed until 50% D_2O in the growth water, as the deviation in doubling time was well within the natural variance. However, after overnight cultivation the OD values became equal between the different incubations and the density of the 100% D_2O cultures reached the same OD values as the control incubations without D_2O.

3.1.3 Influence of heavy water on cell morphology
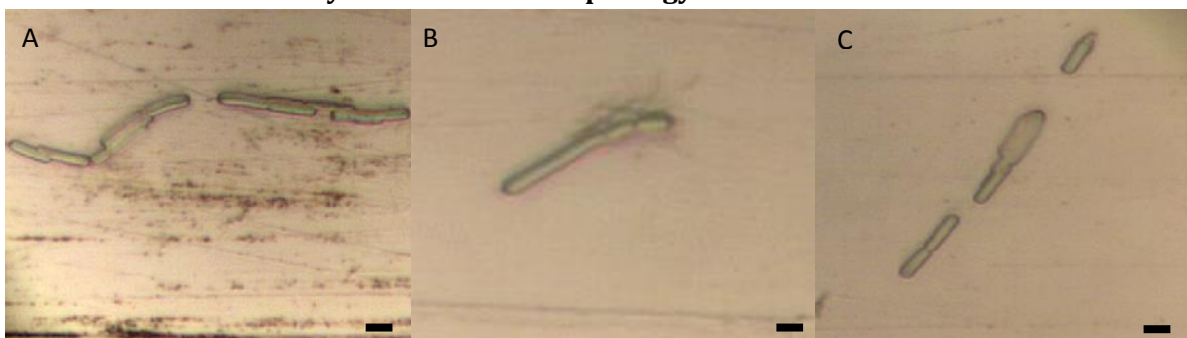

Figure 6: *B. subtilis* grown in LB-medium containing (A) 0%, (B) 50% and (C) 100% D_2O. Cells spotted on aluminum coated slides and recorded with the Raman microscope. Scale bar indicates 2µm.

B. subtilis cells, observed with the Raman microscope, revealed that high concentrations of deuterium in the medium had no considerable influence on the cell morphology. The

cells were rod shaped and had approximately the same size as cells which were grown without D_2O (Fig. 6).

3.2 Effect of Storage and Fluorescence in situ Hybridization (FISH) on deuterium labeled cells in respect to Raman microspectroscopy

3.2.1 Influence of storage conditions on the deuterium label

To ensure that the standard storage conditions (1:1 EtOH:PBS) do not influence the observed deuterium induced peak in Raman microspectroscopy, cells handled following the standard protocol were compared to cells that were left without ethanol.
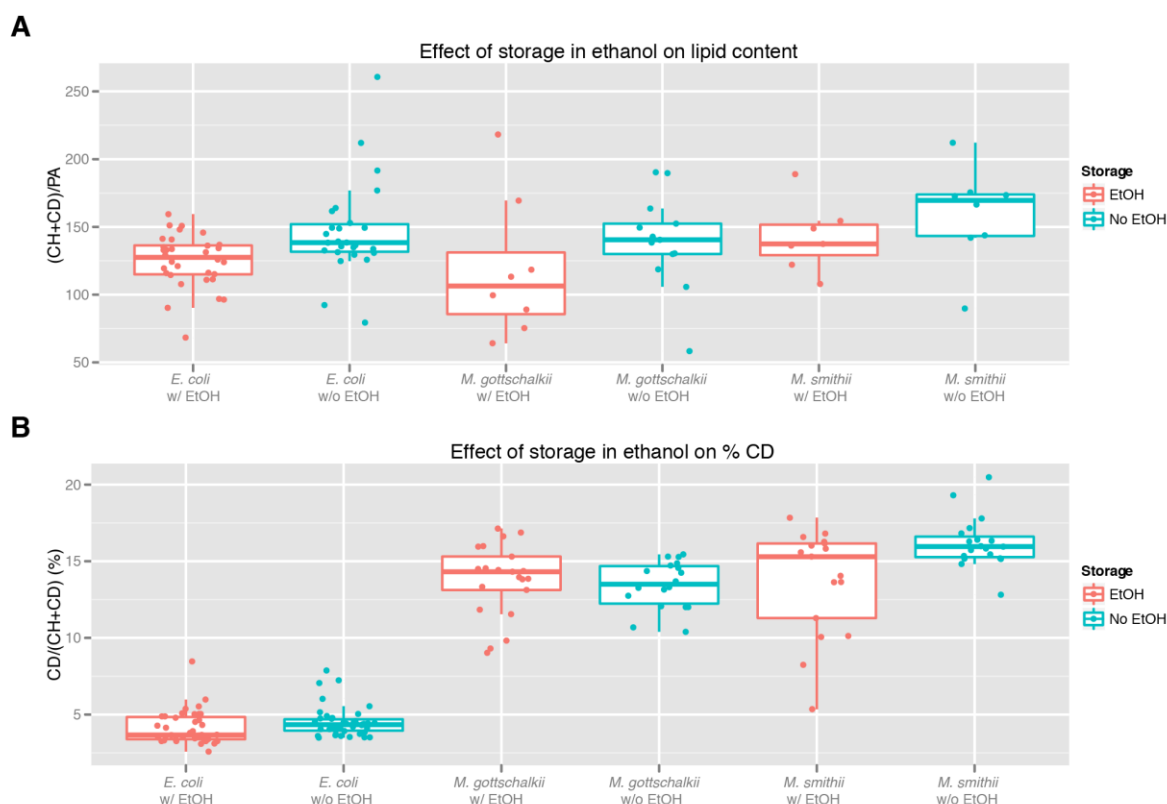
Figure 7: Effect of ethanol storage on deuterium labeled cells. Cultures of *Escherichia coli, Methanobrevibacter gottschalkii,* and *Methanobrevibacter smithii* grown in the presence of 30% D_2O in the growth medium were PFA fixed and stored at 4°C in a 1x PBS solution containing either non or 50% ethanol. Single cell Raman spectra of these cells were compared to evaluate the influence of storage conditions on cellular CH and CD content. Single cell spectra are represented by points and population quartiles are shown as boxplots. (A) The lipid content of the cells was estimated based on the CH + CD content of the cells normalized to the phenylalanine peak height. Approximately 25% of the cellular CH and CD bonds are contributed by lipids and 65% of these bonds are contributed by proteins. (B) %CD was calculated as CD/(CD+CH) (as described in Materials and Methods). Cells stored in the presence of ethanol had a slightly but not significant decreased lipid content and %CD compared to cells stored without ethanol (ANOVA, Tukey HSD test p>0.05) in all tested strains. Graph adapted from Berry et al., 2015.

Differences, as a result of this different treatment on the CD peak of representative species were analyzed. The lipid content (estimated from the CH + CD content normalized to the phenylalanine peak height) and %CD of the respective cells was slightly lower in cells stored in the presence of ethanol (Fig. 7) but this was not

significant (p<0.05). Therefore the standard storage conditions are assumed to be suitable for this isotopic labeling approach.
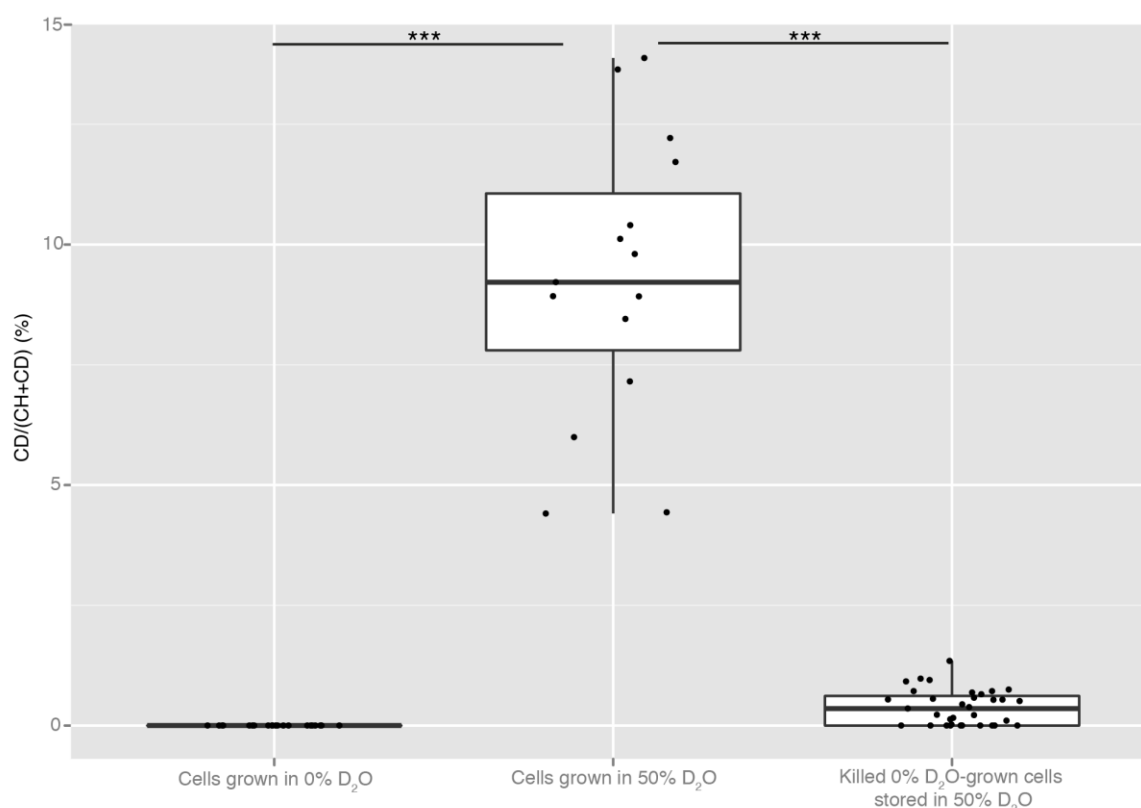

Figure 8: Abiotic hydrogen/deuterium exchange in single cells. *Escherichia coli* **grown without D$_2$O and inactivated by PFA fixation was incubated overnight in 50% D$_2$O. Single cell spectra of these cells were compared to spectra of cells grown without or with 50% D$_2$O in the growth medium. The %CD of the spectra was calculated as described in Materials and Methods. Abiotic exchange was not significant (p=0.58). Each point represents a single cell spectrum and population quartiles are shown as boxplots. ***p<0.001. Graph adapted from Berry et al., 2015.**

To further validate the suitability and reliability of the method a test was conducted to exclude the possibility of abiotic hydrogen/deuterium exchange in the duration of the incubation time. *E. coli* cells grown without D$_2$O and inactivated by PFA fixation were incubated overnight in 50% D$_2$O at 37°C. Raman spectra of these cells were compared to cells grown without or with 50% D$_2$O. A clear distinction between cells grown with 50% D$_2$O or without D$_2$O was visible also the inactivated cells did not assimilate D in a significant quantity (Fig. 8). Therefore the deuterium incorporated in microbes can be considered as solely resulting from cell activity during growth.

3.2.2 Influence of FISH on the lipid content and %CD of cells

The combination of Raman microspectroscopy and FISH was previously already applied on environmental samples to detect substrate utilization patterns in a complex environment (Huang et al., 2007). To evaluate this technique in combination with the deuterium label, *E. coli* cultures grown with 50% D$_2$O were hybridized and the %CD of these samples was compared to cells that had not been subjected to the FISH

procedure. Cells exposed to the FISH protocol exhibited a diminished D label in comparison to non-hybridized cells. To evaluate the cause of this effect and if it is possible to exclude this factor, variations of the hybridization protocol were tested on *E. coli* grown with 50% D_2O. Variations of the liquid FISH protocol (as described in Materials and Methods) to exclude the dehydration (EtOH) step, SDS or formamide as well as
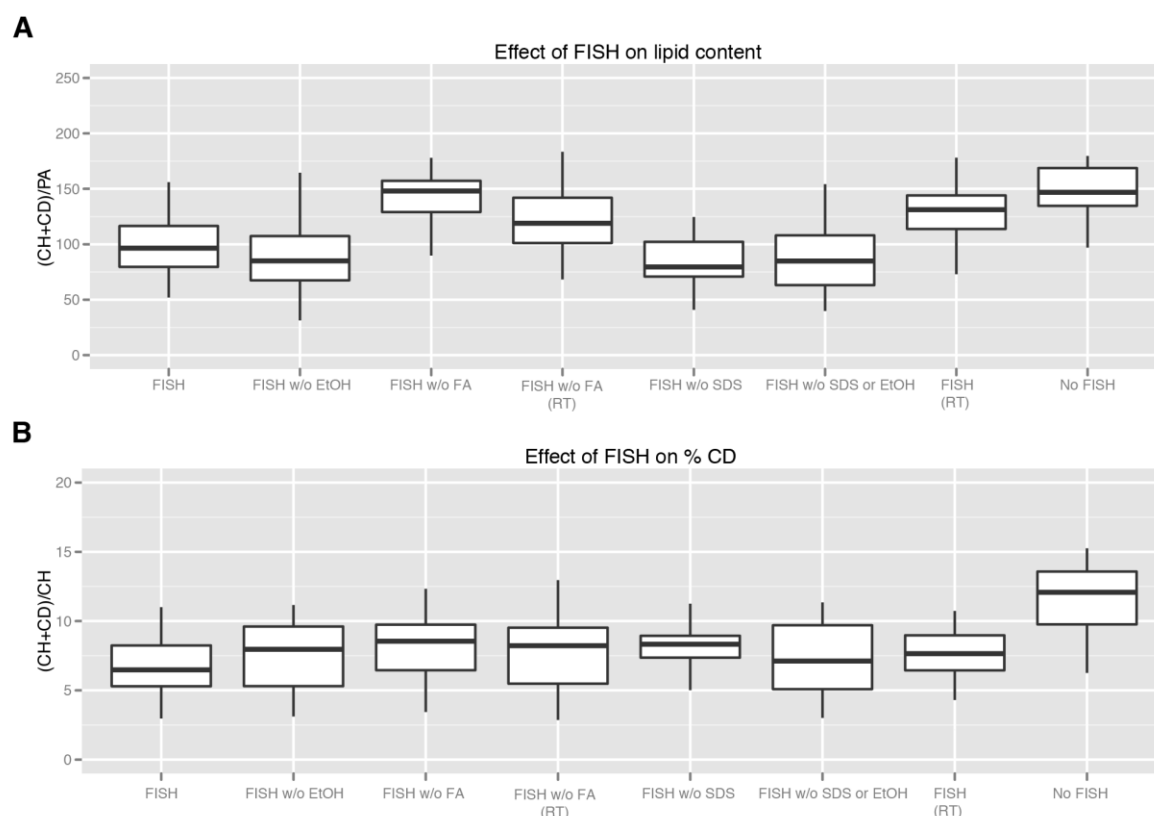

Figure 9: Effect of dehydration and buffer solutions as part of the FISH procedure on the CD and CH peak in Raman spectra of deuterium labeled *Escherichia coli* cells. *E. coli* grown with 50% D_2O in the medium was used for all tested variations of the FISH protocol. Between 25 and 32 cells were measured for each modification. The liquid FISH protocol as described in Materials and Methods was performed and modified to exclude the dehydration (EtOH) step, formamide (FA), sodium dodecyl sulfate (SDS), a combination of these, or hybridization at room temperature (RT) instead of 46°C. Raman spectra of these variations were compared to spectra of cells that had not undergone the hybridization procedure. (A) The lipid content was estimated by calculation of the CD+CH content of the cells normalized to the phenylalanine peak height. (B) %CD was calculated as described in Materials and Methods. All tested variations of the FISH protocol significantly affected the %CD and all variations affected the lipid content except hybridization without formamide and at room temperature (ANOVA, Tukey HSD test: $p<0.05$). Graph adapted from Berry et al., 2015.

hybridization at room temperature were conducted. The lipid content of the cells was equally altered by all variations of the FISH protocol except hybridization without formamide and/or at room temperature instead of 46°C. Less reduction of the lipid content of the cells was observed under these conditions (Fig. 9A). As no specific FISH signals can be achieved in hybridizations without formamide or exact defined temperature, to ensure stringency, the loss of cellular lipids cannot be prevented. Further the analysis of the D incorporation in microbial cells, in this study, is generally

based on the %CD and here no differences between the modifications of the FISH protocol were observed. The %CD was similarly affected by all of the modifications and the average reduction was 42% (Fig. 9B). As the formamide and temperature does not specifically reduce the deuterated lipids, but influences the absolute amount of lipids in the cell, and the %CD is calculated as the ratio of the CD to CH peak area this value is not affected by changes in the hybridization protocol. Therefore a reduction of the D label intensity must be accepted for a Raman-FISH approach.

3.3 Application of the deuterium label on the mouse cecum community

To test the applicability of the labeling method in ecological studies a more complex community was required. Therefore the cecal content of three adult mice was obtained and incubated overnight at 37°C with 50% deuterium oxide in the growth water. Further the incubations were amended with different substrates (glucose, glucosamine, mannose, gastric mucin and nothing as negative control). The cells were harvested and inactivated by PFA fixation to preserve until measurement.

3.3.1 Assimilation of D in the gut community in regard to different substrates

The samples were stained with DAPI and 68-92 single cells of each incubation and population were measured. To detect the overall activity of the gut community in response to the different substrates cells were randomly chosen for measurement. Further two common members of the gut community (*A. muciniphila* and *B. acidifaciens*) were specifically targeted (FISH). The %CD of the randomly chosen cells as well as the specifically targeted populations were compared for all treatments. The addition of glucose (81%), mannose (75%), and mucin (71%) did stimulate a large fraction of the overall community, whereas glucosamine (41%) lead to a less pronounced reaction (Fig. 10B). In the control incubation without any amendment still a small fraction of the community was active (~9%).

3.3.2 Specific activity measurement of *Bacteroides acidifaciens* and *Akkermansia muciniphila*

The combination of Raman and FISH was used to determine the differences in substrate utilization patterns between certain members and the gut community. Cells identified as *B. acidifaciens* were highly stimulated by all added substrates with the highest number of labeled cells in the mannose amended incubation followed by mucin, glucose and glucosamine. In contrast, *A. muciniphila* presented a very distinct specialization. As *A. muciniphila* is a known mucin degrader, the strain was primarily active in the incubation containing 1% mucin as expected. Only low activity was detected in mannose and glucose amendments and no increase in activity compared to the control was found in the glucosamine amendment (p<0.05). While the labeled cells in the glucosamine amended incubation had a relatively high portion of *B. acidifaciens*, the fraction of highly labeled (>10%) cells was notably lower than in the other incubations. *A. muciniphila* on the other hand had no considerable proportion of labeled cells in neither incubation, but an important fraction of highly labeled cells in the mucin amendment (Fig. 10C).
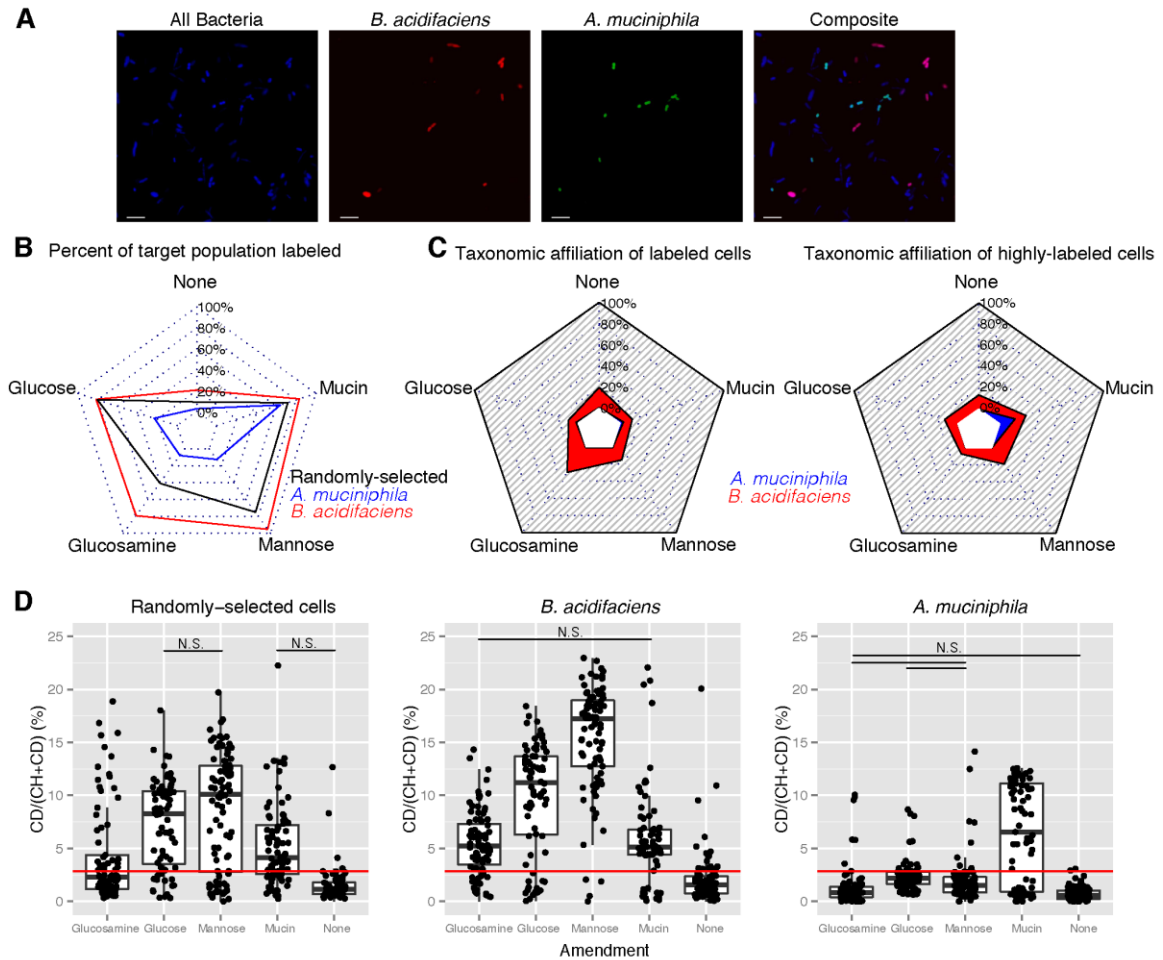
Figure 10: Application of D$_2$O in mouse cecum incubations with various substrates to monitor the activity of microbiota on a single cell level. Experiments were performed on mouse cecum content incubations amended with glucose, glucosamine, mannose, mucin or nothing as a control. (A) FISH images of all Bacteria (blue), *Bacteroides acidifaciens* (red), *Akkermansia muciniphila* (green) and composite. (Scale bar: 5 μm). (B) Percentage of deuterium labeled cells of different populations within the mouse cecal incubation amended with various substrates. Raman measurements of 68-92 cells were performed for each population and substrate. (C) Fraction of FISH targeted cells to all labeled (*Left*) and highly labeled (*Right*, >10%CD) cells in the gut community in the different incubations. These contributions were calculated as follows: [Relative abundance of target population as measured by quantitative FISH using a specific probe] * [Proportion of target population labeled]/[Relative abundance of all labeled cells]. (D) Visualization of deuterium assimilation rate into randomly selected and FISH targeted (*A. muciniphila* and *B. acidifaciens*) cells. Single cell spectra are denoted by black points and population quartiles are shown as boxplots. The red line indicates the threshold to consider a cell as labeled (2.78 %CD), determined by calculating the mean + 3 s.d. of %CD of randomly selected cells incubated without substrate amendment. All comparisons are statistical significant (p<0.05), except when denoted N.S. (not significant). Graph adapted from Berry et al., 2015.

The %CD within the different incubations varied strongly revealing a high heterogeneity within the population (Fig 10D). With exception of the not amended sample all incubations contained highly active as well as non-active cells indicating different populations within the gut community. But also with the focus on a specific species (*B. acidifaciens* or *A. muciniphila*) strong heterogeneity was observed. This is also represented in Figure S4 showing typical Raman spectra of *B. acidifaciens* cells identified by FISH. Cells even from the same species and in close proximity in the sample reacted differently to the addition of glucose. While one cell (red spectra) is clearly labeled with

deuterium the other one (black spectra) has no or a nearly undetectable CD peak.

3.3.3 Determination of the abundance of *A. muciniphila* and *B. acidifaciens*

The composition of the gut community was explored microscopically and the abundance of *B. acidifaciens* and *A. muciniphila* was ascertained by quantification of 60 fields of view (Fig. 10A: representative images of the mouse gut community) of each treatment calculated from the volume fraction of targeted cells within all bacteria. The abundance of *B. acidifaciens* varied between the different incubations with the highest abundance in the glucosamine (14.9%) and mannose (11.2%) amendment followed by the not amended (8.3%), the gastric mucin (7.4%) and the glucose (7.2%) amendment. *A. muciniphila* had in the glucose (7.7%) and mannose (6.0%) amendment the highest abundance close to *B. acidifaciens*, while with glucosamine (4.0%), mucin (3.7%) and no amendment (3.2%) the abundance is lower. Surprisingly while the activity of *A. muciniphila* was highest in the incubation containing gastric mucin the abundance does not increase accordingly, it is not higher than in the control incubation.

4. Discussion

4.1 The application of D_2O in microbiology

4.1.1 The use of deuterium as isotopic marker in Raman microspectroscopy

Methods to study the activity and function of microorganisms in their environment are limited, but essential to understand the complex interactions within an ecosystem. To get insight in metabolic pathways the utilization of stable isotopes was found to be a useful tool. The isotopes are used to explore the ecological function of organisms and as far as possible also the food-web in a complex community. A limitation of these techniques is that they only provide information about specific functional groups and processes in the system. Furthermore the artificial supply of labeled substrate could compromise the activity patterns and community composition by elevated substrate concentrations. To overcome these limitations an unspecific general activity marker is required.

A wide range of studies proved that D_2O is applicable in bacterial cell cultures and preliminary tests with *E. coli*, grown with high concentrations of deuterium, provided first evidence for the possibility to detect deuterium in microbial cells with Raman microspectroscopy (data by Christoph Böhm, not shown). Although numerous studies concerning deuterium exist, so far Raman based studies on deuterium have predominantly investigated the structure of chemical or cellular compounds (Craig et al., 2003; Qiang et al., 2005; Ribeiro-Claro and Teixeira-Dias, 1984). The combination of D_2O as isotopic label for microbial cells in Raman microspectroscopy is a new approach. A major advantage compared to other SIP techniques is that Raman microspectroscopy provides information at a single cell level. Further the method is quick and nondestructive, and therefore it opens the possibility to further manipulate and examine the cells.

4.1.2 The influence of heavy water on the growth rate of bacteria

The isotopic effect of deuterium was studied intensively after its discovery and isolation in the 1930s but waned rapidly as the supply was limited and cost intensive. With the rise of nuclear energy, heavy water was manufactured on a large scale and in the 1960s numerous studies on the biological effect of the isotope were conducted (Borek and Rittenberg, 1960; De Giovanni and Zamenhof, 1963; Lovett, 1964).

In studies on various bacterial strains the isotopic effect of heavy water on the growth and longevity of cells was demonstrated to be diverse. While in the presence of high concentrations of D_2O the lag phase is prolonged and the subsequent logarithmic growth phase is slowed down (De Giovanni, 1960; Lester et al., 1960) also a depletion of deuterium below the natural abundance leads to slower growth (Somlyai et al., 1993). *Aerobacter aerogenes* starving in minimal media with 75% D_2O showed no sign of

toxicity, in contrast it exhibited a prolonged viability under this conditions (Lovett, 1964). Lester et al. (2006) showed for different strains of *Mycobacteria tuberculosis* growth inhibition as well as prolonged survival rates. Also slight stimulatory effects of deuterium in concentrations ranging from 25% to 98% D_2O were reported (Lester et al., 1960; Lu et al., 2013). Further experiments revealed that the biofilm formation of bacteria could be either increased or decreased by D_2O in the medium (Wiberg, 1955). This indicates that cell physiological processes in general are slowed down.

Despite these diverse and strong effects reported for deuterium also adaptation to this isotope was observed. Adapted cultures were able to grow at the same rates as cells in normal medium (Butler and Grist, 1984).

The growth experiments carried out in this study were consistent with the common observation of growth inhibition in deuterated medium (Crespi et al., 1960; De Giovanni, 1960; De Giovanni and Zamenhof, 1963; Hochuli et al., 2000). Non-adapted *E. coli* cultures grown in LB-medium with various concentrations of D_2O indicated that until a growth water substitution of 50% D_2O no significant effect on the growth rate is detectable. The optical density measurements were congruent with this, and were located within the natural variance in all cultures until the deuterium concentration reaches 50%. Exceeding this concentration a slight decrease in growth rate becomes apparent. In 100% D_2O the lag-phase of the cultures did increase recognizably but not to an extent of 24-30h as reported by Borek and Rittenberg (1960) (Fig. 5A). *B. subtilis* revealed a similar pattern with decreased growth rates starting at 50% D_2O (Fig. 5B). In *B. thuringiensis* which was chosen because of a report that *Bacillus cereus*, a close relative of *B. thuringiensis*, is stimulated by high concentrations of D_2O, the decreased growth rate is less pronounced and the doubling time in 100% D_2O is not significantly lower. The observed stimulation of growth of *Bacillus cereus* in deuterated medium with concentrations ranging from 50% to 98% D_2O with the highest growth rate at 75% D_2O (Lu et al., 2013) was not confirmed with *B. thuringiensis* in this study. On the contrary, deuterium oxide amendment did neither stimulate nor decreased the growth of this strain (Fig. 5C).

Butler and Grist (1984) proposed that the toxic effect of D_2O results not just from the isotopic effect of deuterium but instead from the presence of both deuterium and hydrogen together. They hypothesized that the contamination of pure D_2O with H_2O prevents the need for adaptation to occur as it stems from the presence of both deuterated and non-deuterated products in the cell at the same time. The stronger and shorter bonds (different bond angle) to deuterium could lead to an accumulation of deuterons in macromolecules and the mass difference of the isotopes results in the following in conformational changes in the molecules that affect the enzymatic activity and be in part responsible for the observed toxic effect. Contradicting to this is that the same reactions connected to high deuterium concentrations can be observed for

oxidative or osmotic stress (Newo et al., 2004). Interestingly additional repair systems that are not available for non-adapted cells seem to be activated due to deuterium incorporation. This is supported by the significantly higher UV irradiation resistance of adapted cells (Butler and Grist, 1984) which also indicates the availability of repair capabilities not present in non-adapted cells.

In accordance with former studies it can be assumed that concentrations up to 50% D_2O in the growth medium are suitable for labeling experiments. Generally this induces only meager effects on the cell growth which could be either enhancing or inhibiting. At a higher concentration the toxic effect of the isotope would prevail.

4.2 Deuterium in Raman spectroscopy

Deuterium is established in Raman spectroscopy to study chemical structures of complex molecules (Nickolov et al., 1994; Qiang et al., 2005; Ribeiro-Claro and Teixeira-Dias, 1984) and was also found to be suitable as a solvent (Craig et al., 2003).

4.2.1 Detection of deuterated cells with Raman microspectroscopy

The prominent Raman band between 2800-3100 cm^{-1} is assigned to stretching vibrations of CH_2 and CH_3 groups (Krafft et al., 2003; Trumpy, 1935) present in macromolecules including lipids, proteins and nucleic acids. Multiple studies revealed that the main contributor of hydrogen in cellular lipids is water (Sessions et al., 2002; Zhang et al., 2009). Wegener et al. (2012) demonstrated that substitution of water for heavy water leads to a distinct deuteronation of the lipid fraction of cells. Therefore the introduction of deuterium into microbial cells by D_2O should result in deuterated lipids similar to ^{13}C correlated to a shift of the respective Raman band. With this in mind we hypothesized that an exchange of H_2O to D_2O in the growth medium would generate deuterated lipids to be visualized by Raman microspectroscopy.

To test this hypothesis Raman measurements of *E. coli* grown with or without D_2O were conducted. Indeed several shifted peaks were observed in cell spectra of cultures grown in partly or completely substituted growth water. Most recognizably, a broad peak appeared in the region of 2040 to 2300 cm^{-1} where in non-labeled cells no peak is detectable. This region of the Raman spectrum is assigned to CD_x stretching vibrations (Bansil et al., 1980; Bryant et al., 1982; Falk, 1990). The intensities of the deuterium assigned peak of *E. coli* and two additional selected species grown in medium with various D_2O concentrations (summarized in Fig. S1) revealed a constant increase in peak height correlated with deuterium oxide concentration. This was observed consistent in numerous randomly selected cells of all tested species (Fig. 3A). Interestingly at a concentration of 30% D_2O in *B. thuringiensis* the CD peak is more prominent than in *E. coli* or *B. subtilis* (Fig. S1). When the growth medium contained 50% D_2O the peak height equalizes between all selected species. Linked to the growth curves obtained from the tested strains (Fig. 5) it seems that *B. thuringiensis* adapts better, to low concentrations of deuterated water than the other tested species. Nevertheless comparing the variance

between the measured cells within one sample and between the biological replicates this can be considered natural variance. This was also confirmed by repeated measurements on the same cell. Multiple measurements did not reveal discrepancies of the observed label (Fig. S3). This indicated that the CD band around 2200 cm^{-1} is reliable to see D assimilation in bacterial cells and shows that it provides reliable information about the uptake and therefore activity of the cell.

Studied attentively the appearance of the CD band of *E. coli* cells grown in full substituted medium changes and a shoulder on the side of the peak emerges. This shoulder indicates a highly fractionating metabolic pathway which accepts deuterium only if there is no hydrogen available. The peak separation is clearly visible in *E. coli* spectra while in the two *Bacillus* strains only a slight alteration of the CD band appears (Fig. S1), suggesting that the metabolic pathways of the species are not uniformly and the discrimination of deuterium differs. Discrimination of the heavier isotope is widespread in living cells (Campbell et al., 2009; Sessions et al., 2002; Zhang et al., 2009) this was addressed with additional measurements of metabolically diverse strains and is further discussed in the following.

In the spectral region between 1800 and 2800 cm^{-1} although there are no peaks in cells grown without deuterium, irregularities of this region lead to a higher variance in peak area ratio than anticipated. The "dead area" of the Raman spectra is not completely flat, and this may decrease the sensitivity of the deuterium label. One factor affecting the signal to noise ratio is the purity of the sample. Clustered or insufficiently washed cells enclosed by extracellular compounds in some cases result in fluorescence signals. This can mask relevant peaks or introduce bands not originating from the cells and possibly also influences the CD group associated area and leads to variance, as seen in the controls grown without D$_2$O (Fig. S1).

4.2.3 The difference in deuterium assimilation in Auto- and heterotrophic microbes
A study of Wegener et al. (2012) demonstrated that growth water is the main contributor of H in cell lipids. Based on the rate of deuterium incorporation in the cell lipid formation and ^{13}C assimilation he could distinguish between heterotrophic and autotrophic growth. This prompts the question if also with Raman microspectroscopic measurements, as introduced in this study this difference could be observed. To evaluate this possibility tests with different species performing various metabolic functions were performed.

As before, all tested organisms exhibited a peak appearing in the CD region correlated to a reduction of the CH peak indicating that this labeling technique can be applied for diverse organisms. As hypothesized differences in deuterium assimilation rates were found between the heterotrophic bacterial reference strains (*B. subtilis* and *B. thuringiensis*) and the autotrophic methanogenic archaea (*Methanobrevibacter smithii*,

and *Methanocorpusculum labreanum*) grown in the presence of 30% deuterium oxide (Fig. 3).

Lipid biosynthesis is associated with uptake and exchange of water derived protons catalyzed by NADP(H). The Hydrogen in fatty acids derives to 50% from NADP(H) and in addition 25% hydrogen is assimilated directly from water (Sessions et al., 2002; Zhang et al., 2009). Campbell (2009) even proposed that all H in fatty acids derives from water.

Another factor to consider is the difference in membrane composition of microbes. Archaeal cell membranes are built from isoprenoid lipids and are generally D depleted relative to n-alkyl lipids (Zhang et al., 2009) which are the main compound of bacterial cell membranes. Furthermore the archaeal membranes contain a high amount of CH_3 groups in contrast to bacterial membranes which are built primarily from CH_2 groups with minor amounts of CH_3. This difference was used to spectroscopically distinguish between archaeal and bacterial cells in a mixed community (Probst et al., 2013). Another factor to be considered is the discrimination that is known to appear for isotopically mixed substrates. Fractionation of Hydrogen during lipid biosynthesis is different between autotrophs and heterotrophs (Fischer et al., 2013). In several studies it was found that a selective incorporation with a preference for H against D occurs. Further interesting is the fact that this fractionation factor is not consistent between different species. In general heterotrophic growth has a low depletion between water and lipids while autotrophs reveal a high depletion (Fischer et al., 2013; Sessions et al., 2002; Zhang et al., 2009). Additionally a difference of the fractionation factor in different metabolic pathways within one organism was reported as isoprenoid lipids were found to be generally deuterium depleted compared to n-alkyl lipids (Sessions et al., 1999). Fischer et al. (2013) found that in a medium with 4% deuterium the phosphatidyethanolamine lipids of chemoautotrophs were depleted by ~1% (mean deuterium content of ~3%). As most of the experiments focused on a deuterium concentration near the natural abundance of the isotope and the highest fractionation observed was +993‰ (Campbell et al., 2009) and -400‰ (Zhang et al., 2009) the influence of differences in the fractionation factor is neglectable. Nevertheless a difference in assimilation amount between different strains was apparent. While these factors play a more or less important role in the amount of deuterium incorporated in the cell material it is reasonable that the differences observed are primarily based on the metabolic difference of heterotrophic and autotrophic growth.

Heterotrophic organisms grow on diverse substrates which contribute to the cellular mass and will contain some hydrogen while autotrophs are often constrained to water as their only hydrogen source. Therefore, the amount of water derived hydrogen assimilated by these cells is considered to be relatively higher leading to larger amounts of labeled cell compounds. Heterotroph cells on the contrary incorporate hydrogen not only from environmental water but also from the substrate they use for their energy

metabolism. Tests on other strains (*Nitrospira moscoviensis* and *Nitrososphaera gargensis*) performed parallel to this thesis substantiated the findings observed for the presented species (data by Martón Palatinszky and Tae Kwon Lee, not shown).

A quantitative approach with this isotopic labeling technique is in this means not possible as the height of the CD peak is not directly related to the amount of activity the cell conducted. Sessions et al. (2002) found that the hydrogen isotopic composition of lipids did not change between cultures harvested in exponential or stationary phase. He suggested that the membrane lipids lack turn over so that only the isotopic budget during growth is reflected. This is in accordance with our results that cultivation over multiple generations did not increase the amount of deuterium label in bacterial cells, as only the incorporation during the growth phase is accounted for and prolonged growth in deuterated medium does not increase the label intensity (data by Christoph Böhm, not shown).

4.2.4 How does hybridization and storage influence the deuterium label intensity of microbes

The influence of storage and hybridization on the cellular composition and consequently the deuterium content of the labeled cells was a point of concern for the reliability of the isotopic label. To evaluate if the storage conditions influence the observed deuterium induced peak, in Raman microspectroscopy, cells proceeded following the standard protocol (stored in 1:1 EtOH:PBS) were compared to cells left without ethanol. The test showed that the storage does not influence the CD to CH peak area ratio (Fig. 7). Hybridization on the other hand turned out to have an effect on the deuterium label intensity. As shown in Figure 9 the %CD of cells undergone the FISH protocol was significantly reduced (in average 42%) in all modifications tested. The lipid content estimated from the CH+CD content normalized to phenylalanine was less effected when the FISH protocol was performed without formamide and at room temperature, proposing that this are the factors responsible for the loss of cellular D. But as the formamide concentration and temperature are essential factors to obtain specific FISH signals with the DNA oligonucleotide probes it is not suitable to change this in order to prevent the decrease of label intensity when the Raman method is combined with FISH. This will increase the detection limit of the method and is therefore a limitation to be considered. This should be kept in mind for experiments with a low percentage of D_2O but it will also affect studies on low activity organisms.

4.2.2 Determining the detection limit of deuterated cells

As mentioned above, the response of microorganisms to deuterium oxide was investigated in various studies and is not uniform between different species. As expected the %CD variance in all tested species increases with higher concentrations of deuterium. In contrast the interspecies variance decreases with increasing concentrations of D_2O (Fig. S2) this is consistent with the observations made in our growth experiments (Fig. S1). One reason for this could be that the cells adapt at a

divergent pace to the isotope effect and/or not all cells reach simultaneous the same growth stage caused by slightly different growth rates. As seen before, microbial cultures assumed to be homogenous exhibit strong phenotypic heterogeneity leading to heterogeneity in their isotopic composition (Zimmermann et al., 2015). An evaluation with NanoSIMS revealed a similar form of heterogeneity of the cultures examined in this study. All this was more pronounced in cultures with a higher amount of deuterium in the medium (Fig. 4C). As the diversification between the strains is not constant this is considered as stochastic. Therefore, although activity of cells can be seen in all tested strains, a quantification of the activity of the cells in a community is not obtained with this method.

The mathematical detection limit was determined by combining the evaluated detection limit (mean plus 3x s.d. from unlabeled cells) with the linear regression (Fig. S2). This detection limit (16.4%) is in a similar range as the detection limit determined for ^{13}C (~10%) labeled cells (Huang et al., 2007). Further validation of the detection limit in regard of the actual deuterium incorporation into the cell material was carried out with Secondary ion mass spectrometry (NanoSIMS). The amount of deuterium assimilation was found to be substantially lower than the concentration of deuterium in the medium. A growth water concentration of 15% D_2O resulted in only 1.19 at% (mean) deuterium in the cell material of *E. coli* (Fig. 4). This may results in part from fractionation as discussed previous but the discrepancy between growth water concentration and assimilation rate is much higher than observed before in other studies. A comparison of diverse microbes grown in 30% deuterium revealed differences in the assimilation rate of deuterium corresponding with the observed differences in the %CD found in Raman spectra (Fig. 3). The incorporation rate of the heterotrophic bacteria probed in this study were between ~2 and ~4 at% (mean) while in comparison *M. smithii* also grown with 30% D_2O incorporated 8.19 at% (mean) deuterium. Despite this difference in incorporation rate this shows that the utilization of heavy water in combination with Raman microspectroscopy is a sensitive method of stable isotope probing for microbial applications, detecting small fractions of deuterium incorporated into cell material.

4.3 Substrate utilization patterns in the mouse gut community

To explore the possible application in complex environmental studies the mouse gut community was chosen for a proof of principle experiment.

The intestinal tract builds the direct barrier between the animal or human body and the outer environment. The composition of the microbiota colonizing the gut environment is essential to retain the commensal system, and in combination with their richness was suspected to modify cecal compound secretion (Berry et al., 2013). Although the methods are evolving fast and the knowledge is increasing constantly, still the complex nutrient utilization patterns of single microbes are not well understood yet.

The isotopic labeling approach developed in this study was applied on the complex gut microbiome to study the response of microbes to the addition of different substrates. To ensure a reliable label in the Raman microspectrometric measurement 50% of the growth water was supplemented for D_2O and sugars that are components of dietary- and/or host-derived polysaccharides (glucose, glucosamine and mannose) were chosen or for a complex model a mucosal derived glycoprotein (gastric mucin). Microbial cells were probed on a single cell level by Raman microspectroscopy to detect D assimilation. In the first step a non-targeted (randomly selected cells) approach was conducted to explore the activity range of the entire community, followed by a targeted (FISH-based) approach to follow the substrate utilization patterns of two important degraders of host-derived compounds, *A. muciniphila* and *B. acidifaciens* (Arumugam et al., 2011; Berry et al., 2013) (Fig. 10). The comparison of the D assimilation rate of the randomly selected cells showed a vast heterogeneity in the rate of incorporation indicating different populations within the community with different substrate preferences (Fig. 10D). Some active cells were also detected in the not amended sample, due to remaining cecal biomass or decay products of other microbes. This activity baseline (2.78 %CD) is within the range of the before determined detection limit and significantly different to the activity found in the amended incubations. Nevertheless the basic activity of the community has to be considered in order to identify activity directly correlated to a specific substrate.

B. acidifaciens and other *Bacteroides* spp. are versatile in substrate utilization properties as they are able to use a wide range of simple and complex carbohydrates as well as mixed substrates in their metabolism (Miyamoto and Itoh, 2000; Salyers et al., 1977). *A. muciniphila* on the other hand was described as an exclusive mucin degrader using mucin as the sole energy and nitrogen source (Derrien et al., 2004). The abundance and activity patterns of these two species detected in the various incubations were found to be highly dissimilar (Fig. 10) supporting the described metabolic difference between the strains. Referring to the literature the genus *Bacteroides* is the most abundant in the gut microbiome (Arumugam et al., 2011; Weiss and Rettger, 1937) while *Akkermansia* accounts for a fraction of 1 to 3% of the fecal biomass (Derrien et al., 2008). As this value was determined based on fecal samples from humans it is not directly applicable to the experiment performed in this study. Nevertheless, *B. acidifaciens* was generally found in a higher abundance than *A. muciniphila* except in the incubations containing glucose. Further the abundance of *A. muciniphila* was higher than 3% in all of the amendments indicating an attachment of the cells to the mucosal layer of the gastro-intestinal tract to prevent removal. Interestingly, the highest abundance of *A. muciniphila* has been found in the glucose and mannose incubation while the D incorporation rate was similar to the not amended control. The %CD of *A. muciniphila* was as expected high in the incubation containing gastric mucin, but the abundance of the species did not increase accordingly (Fig. 10D). This indicates cell growth without incorporation of D, but referring to the

results obtained in this study this is improbable. One reasons for this inconsistency could be that the abundance in the mucin amended samples is not directly comparable to the other incubations as the experiment was partly repeated and the basic community composition between different mice can vary strongly. Furthermore, *A. muciniphila* grown in mucin medium was observed to be covered in filaments (Derrien et al., 2004) which may influence the FISH. Therefore mucin amendment possibly makes the cells less permeable, and reduces the FISH signals. To test these suggestions additional tests on samples containing mucin would be necessary. In the incubations containing other substrates (glucose, mannose, glucosamine) merely any activity of these cells was detected despite growth was observed before with glucose and N-acetylglucosamine (Derrien et al., 2004). Despite being specialized on the degradation of mucin *A. muciniphila* has a phosphotransferase transporter system (van Passel et al., 2011) providing the capability to utilizing some simple sugars like glucose, glucosamine and mannose. However the data provided in this study do not support this suggestion as this organism was almost exclusively stimulated by mucin (Fig. 10C and D). Mucin stimulated both *B. acidifaciens* and *A. muciniphila.* But in contrast to *A. muciniphila* which is considered a main mucin degrader of the intestinal tract *B. acidifaciens* is more versatile in its nutrient utilization. This difference is demonstrated in the FISH-based approach which was used to profile the activity patterns of the two selected strains based on the introduced D label. While *B. acidifaciens* accounted for 7-19% of all highly labeled cells in all amendments (cells that had >10%CD) *A. muciniphila* represented 15% of highly labeled cells in the mucin amendment but less than 1% in all other incubations (Fig. 10C). This demonstrated that, the amendment of various substrates stimulated predominantly unidentified members of the microbial community despite *B. acidifaciens* and *A. muciniphila* contributed significantly to the community activity.

The experiments demonstrated the applicability of D_2O as isotopic label not only in pure cultures but also in a complex environment to reveal the response of microbes to the amendment of diverse substrates. Further, the combination of Raman microspectroscopy and FISH allows displaying specific species in context to substrate utilization. Hence, some specific metabolic properties of *B. acidifaciens* and *A. muciniphila* could be highlighted in the present study.

For biological application the possibility in Raman spectroscopy to investigate fixed as well as living cells, and the fact that it is nondestructive and therefore further processing of the sample is possible opens prospect for advanced ecological studies.

A possible expansion in the future would be the combination with Laser tweezers for optical trapping of single cells or colonies based on Raman peaks. This could be used for sorting of uncultured species that were identified as active or growing on a specific substrate and further analyze these with single cell genomics, or use them as inoculum for cell cultures.

5. Abstract

Microbial communities are vital for the function of all ecosystems. Nevertheless the knowledge about their complex interactions and dependencies is limited. Methods to study the metabolism and activity patterns of microbes independent from isolation and cultivation are often based on the amendment with isotopically labeled substrates in combination with molecular techniques.

In this study the application of deuterium oxide (D_2O) as a general activity marker in combination with Raman microspectroscopy was tested. The incorporation of heavy isotopes leads to a shift of the corresponding peak in Raman spectra. Initial experiments with various pure cultures grown in the presence of different concentrations of D_2O showed a clear and reproducible red shift of the (mostly lipid related) Carbon-Hydrogen bond peak induced by D_2O. The intensity of this signature CD peak in the Raman spectra was correlated to the D_2O concentration in the growth water, and the incorporation of the isotope in the microbial cell mass was also confirmed by NanoSIMS measurements. These showed that 0.17 at% D in the cell mass is sufficient for the detection of labeled cells. This corresponds to a detection limit below 8 %CD in Raman spectra of all tested strains. As D_2O was often observed to have a toxic effect on living cells, the influence of different concentrations of D_2O on cell growth was investigated. Growth curves of three bacterial strains demonstrated that up to a concentration of 50% D_2O in the growth medium no significant inhibition occurs. The reaction to the addition of D_2O to the growth medium was not consistent for all species, and the autotrophic archaea had a considerable higher incorporation rate compared to the heterotrophic bacteria. This can be explained by the fact that while autotrophic organisms derive all hydrogen from water, heterotrophic cells incorporate additional hydrogen from different substrates. As a consequence exact quantification of activity based on the CD peak is not possible. To further evaluate the reliability of the approach, tests concerning the storage stability and the influence of the FISH protocol on the deuterium label were conducted. While the storage had no significant influence on the intensity of the D label the FISH procedure decreased the %CD at an average of 42%.

In a proof of principle experiment the mouse cecum community was incubated with 50% D_2O and amended with different substrates. The activity within the community could be observed and actively growing cells were identified. Further the possibility of detecting different metabolic pathways in a complex community was demonstrated by combining Raman measurements with D_2O and other specific substrates. *A. muciniphila* and *B. acidifaciens* were specifically targeted with FISH and their response to the amendment of the different substrates was detected. While *B. acidifaciens* was stimulated equally by all substrates *A. muciniphila* was nearly exclusively stimulated by the addition of mucin. This supports the differences in substrate utilization patterns reported for these species. These results demonstrate the successful establishment of a protocol to detect D

assimilation from D_2O in microbial cells of a diverse community by Raman microspectroscopy.

6. Zusammenfassung

Mikrobielle Gemeinschaften sind essentiell für die Funktion aller Ökosysteme, dennoch ist das Wissen über ihre komplexen Interaktionen und Abhängigkeiten begrenzt. Methoden um den Metabolismus und die Aktivität von Mikroorganismen, unabhängig von Isolierung und Kultivierung zu untersuchen basieren oft auf der Zugabe von isotopenmarkierten Substraten in Kombination mit molekularen Techniken.

Im Zuge dieser Studie wurde die Verwendbarkeit von Deuteriumoxid (D_2O) als genereller Aktivitätsmarker in Kombination mit Raman Mikrospektroskopie getestet. Die Einlagerung von schweren Isotopen führt zu einer Verschiebung der entsprechenden Peaks in den Raman Spektren. Erste Experimente mit bakteriellen Reinkulturen, gezüchtet in Medium mit verschiedenen D_2O Konzentrationen zeigten eine deutliche und reproduzierbare Verschiebung des Kohlenwasserstoffbindungen zugeschriebenen Peaks. Die Intensität dieses spezifischen CD Peaks in den Raman Spektren korrelierte mit der D_2O Konzentration im Umgebungswasser. Die Aufnahme des Isotops in die Zellmasse wurde zusätzlich mit NanoSIMS Messungen bestätigt welche zeigten, dass 0,17 at% Deuterium in der Zellmasse ausreichen um markierte Zellen nachzuweisen. Dies entspricht einem Detektionlimit von unter 8 %CD in den Raman Spektren von allen getesteten Spezies. D_2O wurde oft als toxisch für Zellen beobachtet, daher wurde der Einfluss des Isotops auf das Zellwachstum ermittelt. Wachstumskurven von drei bakteriellen Stämmen zeigten, dass bis zu einer Konzentration von 50% D_2O des Umgebungswassers keine signifikante Reduktion des Zellwachstums festgestellt werden kann. Die Reaktion auf die Zugabe von D_2O in das Wachstumsmedium war nicht konsistent für alle Spezies, die autotrophen Archaeen wiesen eine deutlich höhere Assimilationsrate auf als die heterotrophen Bakterienstämme. Dies kann dadurch erklärt werden, dass während autotrophe Organismen den gesamten Wasserstoff direkt aus dem Wasser beziehen, heterotrophe Zellen zusätzlich Wasserstoff von verschiedenen Substraten aufnehmen. In Folge dessen ist eine exakte Quantifizierung der Aktivität, basierend auf der D-Markierung nicht möglich. Zur weiteren Evaluierung der Verlässlichkeit der Methode wurde die Lagerungsstabilität und der Einfluss der Fluoreszenz in situ Hybridisierung auf die Intensität der D-Markierung untersucht. Während die Lagerung keinen signifikanten Einfluss hatte, führte die Hybridisierung zu einer Verringerung der Intensität der D-Markierung von durchschnittlich 42%.

Die Anwendbarkeit dieses Prinzips wurde anhand der Darmflora von Mäusen getestet, welche mit 50% D_2O und verschiedenen Substraten inkubiert wurde. Die Aktivität innerhalb der Gemeinschaft konnte so beobachtet und aktiv wachsende Zellen identifiziert werden. Zusätzlich wurde die Möglichkeit verschiedene Stoffwechselwege innerhalb der Gemeinschaft nachzuweisen, durch die Kombination von Raman Messungen mit D_2O und verschiedenen spezifischen Substraten demonstriert. *A. muciniphila* und *B. acidifaciens* wurden gezielt mittels FISH ausgewält und ihre Reaktion auf die Zugabe der Substrate verfolgt. Während *B. acidifaciens* von allen zugegeben

Substraten gleichermaßen stimuliert wurde, wurde *A. muciniphila* fast ausschließlich durch die Zugabe von Mucin angeregt. Das ist konsistent mit Berichten zur unterschiedlichen Nährstoffverwertung dieser Arten. Diese Ergebnisse demonstrieren die erfolgreiche Entwicklung eines Protokolls zur Detektion der Deuteriumassimilation aus D_2O in Mikroorganismen in komplexen Gemeinschaften mittels Raman Mikrospektroskopie.

7. References

Aanderud, Z.T., and Lennon, J.T. (2011). Validation of heavy-water stable isotope probing for the characterization of rapidly responding soil bacteria. Appl. Environ. Microbiol. *77*, 4589–4596.

Albert, M.J., Mathan, V.I., and Baker, S.J. (1980). Vitamin B12 synthesis by human small intestinal bacteria. Nature *283*, 781–782.

Alexandrino, M., Knief, C., and Lipski, A. (2001). Stable-Isotope-Based Labeling of Styrene-Degrading Microorganisms in Biofilters. Appl. Environ. Microbiol. *67*, 4796–4804.

Arumugam, M., Raes, J., Pelletier, E., Le Paslier, D., Yamada, T., Mende, D.R., Fernandes, G.R., Tap, J., Bruls, T., Batto, J.-M., et al. (2011). Enterotypes of the human gut microbiome. Nature *473*, 174–180.

Bansil, R., Day, J., Meadows, M., Rice, D., and Oldfield, E. (1980). Laser Raman spectroscopic study of specifically deuterated phospholipid bilayers. Biochemistry (Mosc.) *19*, 1938–1943.

Berry, D., Stecher, B., Schintlmeister, A., Reichert, J., Brugiroux, S., Wild, B., Wanek, W., Richter, A., Rauch, I., Decker, T., et al. (2013). Host-compound foraging by intestinal microbiota revealed by single-cell stable isotope probing. Proc. Natl. Acad. Sci. *110*, 4720–4725.

Berry, D., Mader, E., Lee, T.K., Woebken, D., Wang, Y., Zhu, D., Palatinszky, M., Schintlmeister, A., Schmid, M.C., Hanson, B.T., et al. (2015). Tracking heavy water (D2O) incorporation for identifying and sorting active microbial cells. Proc. Natl. Acad. Sci. U. S. A. *112*, E194–E203.

Böhm, C. (2012). Characterization of ammonia-oxidizing archaea by Raman microspectroscopy. Diplomarbeit. Universität Wien.

Bohning, J.J., Misra, T.N., and Choudhury, M. (1998). The Raman Effect (American Chemical Society, national Historic Chemical Landmarks).

Borek, E., and Rittenberg, D. (1960). Anomalous Growth of Microorganisms Produced by Changes in Isotopes in Their Environment. Proc. Natl. Acad. Sci. *46*, 777–782.

Boschker, H.T.S., and Middelburg, J.J. (2002). Stable isotopes and biomarkers in microbial ecology. FEMS Microbiol. Ecol. *40*, 85–95.

Bryant, G.J., Lavialle, F., and Levin, I.W. (1982). Effects of membrane bilayer reorganizations on the 2103 cm−1 Raman spectral C␣D stretching mode linewidths in dimyristoyl phosphatidylcholine-d54 (DMPC-d54) liposomes. J. Raman Spectrosc. *12*, 118–121.

Buckley, D.H., Huangyutitham, V., Hsu, S.-F., and Nelson, T.A. (2007). Stable Isotope Probing with 15N Achieved by Disentangling the Effects of Genome G+C Content and Isotope Enrichment on DNA Density. Appl. Environ. Microbiol. *73*, 3189–3195.

Butler, L.O., and Grist, R.W. (1984). The Effect of D2O on the Growth and Transforming Activities of Streptococcus pneumoniae. J. Gen. Microbiol. *130*, 483–494.

Campbell, B.J., Li, C., Sessions, A.L., and Valentine, D.L. (2009). Hydrogen isotopic fractionation in lipid biosynthesis by H2-consuming Desulfobacterium autotrophicum. Geochim. Cosmochim. Acta *73*, 2744–2757.

Craig, N.C., Fuchsman, W.H., and Lacuesta, N.N. (2003). Investigation of Model Cell Membranes with Raman Spectroscopy: A Biochemistry Laboratory Experiment. J. Chem. Educ. *80*, 1282.

Crespi, H.L., Conrad, S.M., Uphaus, R.A., and Katz, J.J. (1960). Cultivation of Microorganisms in Heavy Water. Ann. N. Y. Acad. Sci. *84*, 648–666.

Daims, H., Lücker, S., and Wagner, M. (2006). daime, a novel image analysis program for microbial ecology and biofilm research. Environ. Microbiol. *8*, 200–213.

Dave, M., Higgins, P.D., Middha, S., and Rioux, K.P. (2012). The human gut microbiome: current knowledge, challenges, and future directions. Transl. Res. *160*, 246–257.

Derrien, M., Vaughan, E.E., Plugge, C.M., and Vos, W.M. de (2004). Akkermansia muciniphila gen. nov., sp. nov., a human intestinal mucin-degrading bacterium. Int. J. Syst. Evol. Microbiol. *54*, 1469–1476.

Derrien, M., Collado, M.C., Ben-Amor, K., Salminen, S., and de Vos, W.M. (2008). The Mucin degrader Akkermansia muciniphila is an abundant resident of the human intestinal tract. Appl. Environ. Microbiol. *74*, 1646–1648.

Doré, J., and Corthier, G. (2010). The human intestinal microbiota. Gastroentérologie Clin. Biol. *34*, S7–S15.

Eckburg, P.B., Bik, E.M., Bernstein, C.N., Purdom, E., Dethlefsen, L., Sargent, M., Gill, S.R., Nelson, K.E., and Relman, D.A. (2005). Diversity of the Human Intestinal Microbial Flora. Science *308*, 1635–1638.

Falk, M. (1990). Frequencies of H-O-H, H-O-D and D-O-D bending fundamentals in liquid water. J. Raman Spectrosc. *21*, 563–567.

Fischer, C.R., Bowen, B.P., Pan, C., Northen, T.R., and Banfield, J.F. (2013). Stable-Isotope Probing Reveals That Hydrogen Isotope Fractionation in Proteins and Lipids in a Microbial Community Are Different and Species-Specific. ACS Chem. Biol. *8*, 1755–1763.

Galand, P.E., Casamayor, E.O., Kirchman, D.L., and Lovejoy, C. (2009). Ecology of the rare microbial biosphere of the Arctic Ocean. Proc. Natl. Acad. Sci. *106*, 22427–22432.

Gill, S.R., Pop, M., DeBoy, R.T., Eckburg, P.B., Turnbaugh, P.J., Samuel, B.S., Gordon, J.I., Relman, D.A., Fraser-Liggett, C.M., and Nelson, K.E. (2006). Metagenomic Analysis of the Human Distal Gut Microbiome. Science *312*, 1355–1359.

De Giovanni, R. (1960). The Effects of Deuterium Oxide on Certain Microorganisms. Ann. N. Y. Acad. Sci. *84*, 644–647.

De Giovanni, R., and Zamenhof, S. (1963). Studies on incorporation of deuterium into bacteria. Biochem. J. *87*, 79–82.

Haferkamp, I., Schmitz-Esser, S., Wagner, M., Neigel, N., Horn, M., and Neuhaus, H.E. (2006). Tapping the nucleotide pool of the host: novel nucleotide carrier proteins of Protochlamydia amoebophila. Mol. Microbiol. *60*, 1534–1545.

Haider, S., Wagner, M., Schmid, M.C., Sixt, B.S., Christian, J.G., Häcker, G., Pichler, P., Mechtler, K., Müller, A., Baranyi, C., et al. (2010). Raman microspectroscopy reveals long-term extracellular activity of chlamydiae. Mol. Microbiol. *77*, 687–700.

Harz, M., Rösch, P., and Popp, J. (2009). Vibrational spectroscopy—A powerful tool for the rapid identification of microbial cells at the single-cell level. Cytometry A *75A*, 104–113.

Hochuli, M., Szyperski, T., and Wüthrich, K. (2000). Deuterium isotope effects on the central carbon metabolism of Escherichia coli cells grown on a D2O-containing minimal medium. J. Biomol. NMR *17*, 33–42.

Huang, W.E., Griffiths, R.I., Thompson, I.P., Bailey, M.J., and Whiteley, A.S. (2004). Raman Microscopic Analysis of Single Microbial Cells. Anal. Chem. *76*, 4452–4458.

Huang, W.E., Stoecker, K., Griffiths, R., Newbold, L., Daims, H., Whiteley, A.S., and Wagner, M. (2007). Raman-FISH: combining stable-isotope Raman spectroscopy and fluorescence in situ hybridization for the single cell analysis of identity and function. Environ. Microbiol. *9*, 1878–1889.

Huang, W.E., Ferguson, A., Singer, A.C., Lawson, K., Thompson, I.P., Kalin, R.M., Larkin, M.J., Bailey, M.J., and Whiteley, A.S. (2009). Resolving Genetic Functions within Microbial Populations: In Situ Analyses Using rRNA and mRNA Stable Isotope Probing Coupled with Single-Cell Raman-Fluorescence In Situ Hybridization. Appl. Environ. Microbiol. *75*, 234–241.

Krafft, C., Knetschke, T., Siegner, A., Funk, R.H.W., and Salzer, R. (2003). Mapping of single cells by near infrared Raman microspectroscopy. Vib. Spectrosc. *32*, 75–83.

De Laeter, J.R., Böhlke, J.K., De, B.P., Hidaka, H., Peiser, H.S., Rosman, K.J.R., and Taylor, P.D.P. (2009). Atomic weights of the elements. Review 2000 (IUPAC Technical Report). Pure Appl. Chem. *75*, 683–800.

Lester, W., Sun, S.H., and Seber, A. (1960). Observations on the Influence of Deuterium on Bacterial Growth. Ann. N. Y. Acad. Sci. *84*, 667–677.

Li, M., Huang, W.E., Gibson, C.M., Fowler, P.W., and Jousset, A. (2013). Stable Isotope Probing and Raman Spectroscopy for Monitoring Carbon Flow in a Food Chain and Revealing Metabolic Pathway. Anal. Chem. *85*, 1642–1649.

Lovett, S. (1964). Effect of Deuterium on Starving Bacteria. Nature *203*, 429–430.

Lu, M.-F., Zhang, Yue-Jie, and Zhang, Hong-Yu (2013). Isotope effects on cell growth and sporulation, and spore heat resistance, survival and spontaneous mutation of Bacillus cereus by deuterium oxide culture. Afr. J. Microbiol. Res. pp. 604–611.

Van Manen, H.-J., Lenferink, A., and Otto, C. (2008). Noninvasive imaging of protein metabolic labeling in single human cells using stable isotopes and Raman microscopy. Anal. Chem. *80*, 9576–9582.

Miyamoto, Y., and Itoh, K. (2000). Bacteroides acidifaciens sp. nov., isolated from the caecum of mice. Int. J. Syst. Evol. Microbiol. *50*, 145–148.

Monod, J. (1949). The Growth of Bacterial Cultures. Annu. Rev. Microbiol. *3*, 371–394.

Montoya, J.P., Holl, C.M., Zehr, J.P., Hansen, A., Villareal, T.A., and Capone, D.G. (2004). High rates of N2 fixation by unicellular diazotrophs in the oligotrophic Pacific Ocean. Nature *430*, 1027–1032.

Newo, A.N.S., Pshenichnikova, A.B., Skladnev, D.A., and Shvets, V.I. (2004). Deuterium Oxide as a Stress Factor for the Methylotrophic Bacterium Methylophilus sp. B-7741. Microbiology *73*, 139–142.

Nickolov, Z.S., Earnshaw, J.C., McGarvey, J.J., and Georgiev, G.M. (1994). Raman study of dioxane–D2O mixtures by analysis of the O–D band structure. J. Raman Spectrosc. *25*, 837–844.

Olgun, A. (2007). Biological effects of deuteronation: ATP synthase as an example. Theor. Biol. Med. Model. *4*, 9.

Ong, S.-E., Blagoev, B., Kratchmarova, I., Kristensen, D.B., Steen, H., Pandey, A., and Mann, M. (2002). Stable Isotope Labeling by Amino Acids in Cell Culture, SILAC, as a Simple and Accurate Approach to Expression Proteomics. Mol. Cell. Proteomics *1*, 376–386.

Osborn, M., and Smith, C. (2004). Molecular Microbial Ecology (Taylor & Francis).

Van Passel, M.W.J., Kant, R., Zoetendal, E.G., Plugge, C.M., Derrien, M., Malfatti, S.A., Chain, P.S.G., Woyke, T., Palva, A., de Vos, W.M., et al. (2011). The Genome of Akkermansia muciniphila, a Dedicated Intestinal Mucin Degrader, and Its Use in Exploring Intestinal Metagenomes. PLoS ONE *6*, e16876.

Pester, M., Bittner, N., Deevong, P., Wagner, M., and Loy, A. (2010). A "rare biosphere" microorganism contributes to sulfate reduction in a peatland. ISME J. *4*, 1591–1602.

Petry, R., Schmitt, M., and Popp, J. (2003). Raman Spectroscopy—A Prospective Tool in the Life Sciences. ChemPhysChem *4*, 14–30.

Probst, A.J., Holman, H.-Y.N., DeSantis, T.Z., Andersen, G.L., Birarda, G., Bechtel, H.A., Piceno, Y.M., Sonnleitner, M., Venkateswaran, K., and Moissl-Eichinger, C. (2013). Tackling the minority: sulfate-reducing bacteria in an archaea-dominated subsurface biofilm. ISME J. *7*, 635–651.

Qiang, S., Hai-Fei, Z., and Ti-Yu, D. (2005). Effects of Temperature on D2O Water Structure Investigated by Raman Spectroscopy. Chin. Phys. Lett. *22*, 661.

Qin, J., Li, R., Raes, J., Arumugam, M., Burgdorf, K.S., Manichanh, C., Nielsen, T., Pons, N., Levenez, F., Yamada, T., et al. (2010). A human gut microbial gene catalogue established by metagenomic sequencing. Nature *464*, 59–65.

Radajewski, S., Ineson, P., Parekh, N.R., and Murrell, J.C. (2000). Stable-isotope probing as a tool in microbial ecology. Nature *403*, 646–649.

Raman, C.V., and Krishnan, K.S. (1928). A new class of spectra due to secondary radiation Part I. Indian J. Phys. *2*, 399–419.

Ribeiro-Claro, P.J.A., and Teixeira-Dias, J.J.C. (1984). The individual CH bond as a Raman spectroscopic probe to the internal rotation of the CHCl2 Group in C6H5CHCl2. J. Raman Spectrosc. *15*, 224–231.

Roh, H., Yu, C.-P., Fuller, M.E., and Chu, K.-H. (2009). Identification of Hexahydro-1,3,5-trinitro-1,3,5-triazine-Degrading Microorganisms via 15N-Stable Isotope Probing. Environ. Sci. Technol. *43*, 2505–2511.

Salyers, A.A., Vercellotti, J.R., West, S.E., and Wilkins, T.D. (1977). Fermentation of mucin and plant polysaccharides by strains of Bacteroides from the human colon. Appl. Environ. Microbiol. *33*, 319–322.

Sessions, A.L., Burgoyne, T.W., Schimmelmann, A., and Hayes, J.M. (1999). Fractionation of hydrogen isotopes in lipid biosynthesis. Org. Geochem. *30*, 1193–1200.

Sessions, A.L., Jahnke, L.L., Schimmelmann, A., and Hayes, J.M. (2002). Hydrogen isotope fractionation in lipids of the methane-oxidizing bacterium Methylococcus capsulatus. Geochim. Cosmochim. Acta *66*, 3955–3969.

Sixt, B.S., Siegl, A., Müller, C., Watzka, M., Wultsch, A., Tziotis, D., Montanaro, J., Richter, A., Schmitt-Kopplin, P., and Horn, M. (2013). Metabolic Features of Protochlamydia amoebophila Elementary Bodies – A Link between Activity and Infectivity in Chlamydiae. PLoS Pathog *9*, e1003553.

Sogin, M.L., Morrison, H.G., Huber, J.A., Welch, D.M., Huse, S.M., Neal, P.R., Arrieta, J.M., and Herndl, G.J. (2006). Microbial diversity in the deep sea and the underexplored "rare biosphere." Proc. Natl. Acad. Sci. *103*, 12115–12120.

Somlyai, G., Jancsó, G., Jákli, G., Vass, K., Barna, B., Lakics, V., and Gaál, T. (1993). Naturally occurring deuterium is essential for the normal growth rate of cells. FEBS Lett. *317*, 1–4.

Tap, J., Mondot, S., Levenez, F., Pelletier, E., Caron, C., Furet, J.-P., Ugarte, E., Muñoz-Tamayo, R., Paslier, D.L.E., Nalin, R., et al. (2009). Towards the human intestinal microbiota phylogenetic core. Environ. Microbiol. *11*, 2574–2584.

Trumpy, B. (1935). Raman Spectra of some Deuterium Compounds : Abstract : Nature.

Tulis, J.J., and Eigelsbach, H.T. (1970). Isolation and Properties of a Deuterium-Tolerant Mutant of Pasteurella tularensis. Infect. Immun. *1*, 56–60.

Turroni, F., Ribbera, A., Foroni, E., van Sinderen, D., and Ventura, M. (2008). Human gut microbiota and bifidobacteria: from composition to functionality. Antonie Van Leeuwenhoek *94*, 35–50.

Wagner, M. (2009). Single-Cell Ecophysiology of Microbes as Revealed by Raman Microspectroscopy or Secondary Ion Mass Spectrometry Imaging. Annu. Rev. Microbiol. *63*, 411–429.

Wagner, M., Nielsen, P.H., Loy, A., Nielsen, J.L., and Daims, H. (2006). Linking microbial community structure with function: fluorescence in situ hybridization-microautoradiography and isotope arrays. Curr. Opin. Biotechnol. *17*, 83–91.

Walrafen, G.E. (1973). Weak Raman bands from water. J. Chem. Phys. *59*, 2646.

Walter, J., and Ley, R. (2011). The Human Gut Microbiome: Ecology and Recent Evolutionary Changes. Annu. Rev. Microbiol. *65*, 411–429.

Wegener, G., Bausch, M., Holler, T., Thang, N.M., Prieto Mollar, X., Kellermann, M.Y., Hinrichs, K.-U., and Boetius, A. (2012). Assessing sub-seafloor microbial activity by combined stable isotope probing with deuterated water and 13C-bicarbonate. Environ. Microbiol. *14*, 1517–1527.

Weiss, J.E., and Rettger, L.F. (1937). The Gram-negative Bacteroides of the Intestine. J. Bacteriol. *33*, 423–434.

Wiberg, K.B. (1955). The Deuterium Isotope Effect. Chem. Rev. *55*, 713–743.

Ye, X., Luke, B., Andresson, T., and Blonder, J. (2009). 18O Stable Isotope Labeling in MS-based Proteomics. Brief. Funct. Genomic. Proteomic. *8*, 136–144.

Zhang, X., Gillespie, A.L., and Sessions, A.L. (2009). Large D/H variations in bacterial lipids reflect central metabolic pathways. Proc. Natl. Acad. Sci. *106*, 12580–12586.

Zimmermann, M., Escrig, S., Hübschmann, T., Kirf, M., Brand, A., Inglis, R.F., Musat, N., Müller, S., Meibom, A., Ackermann, M., et al. (2015). Phenotypic heterogeneity in metabolic traits among single cells of a rare bacterial species in its natural environment quantified with a combination of flow cell sorting and NanoSIMS. Microb. Physiol. Metab. *6*, 243.
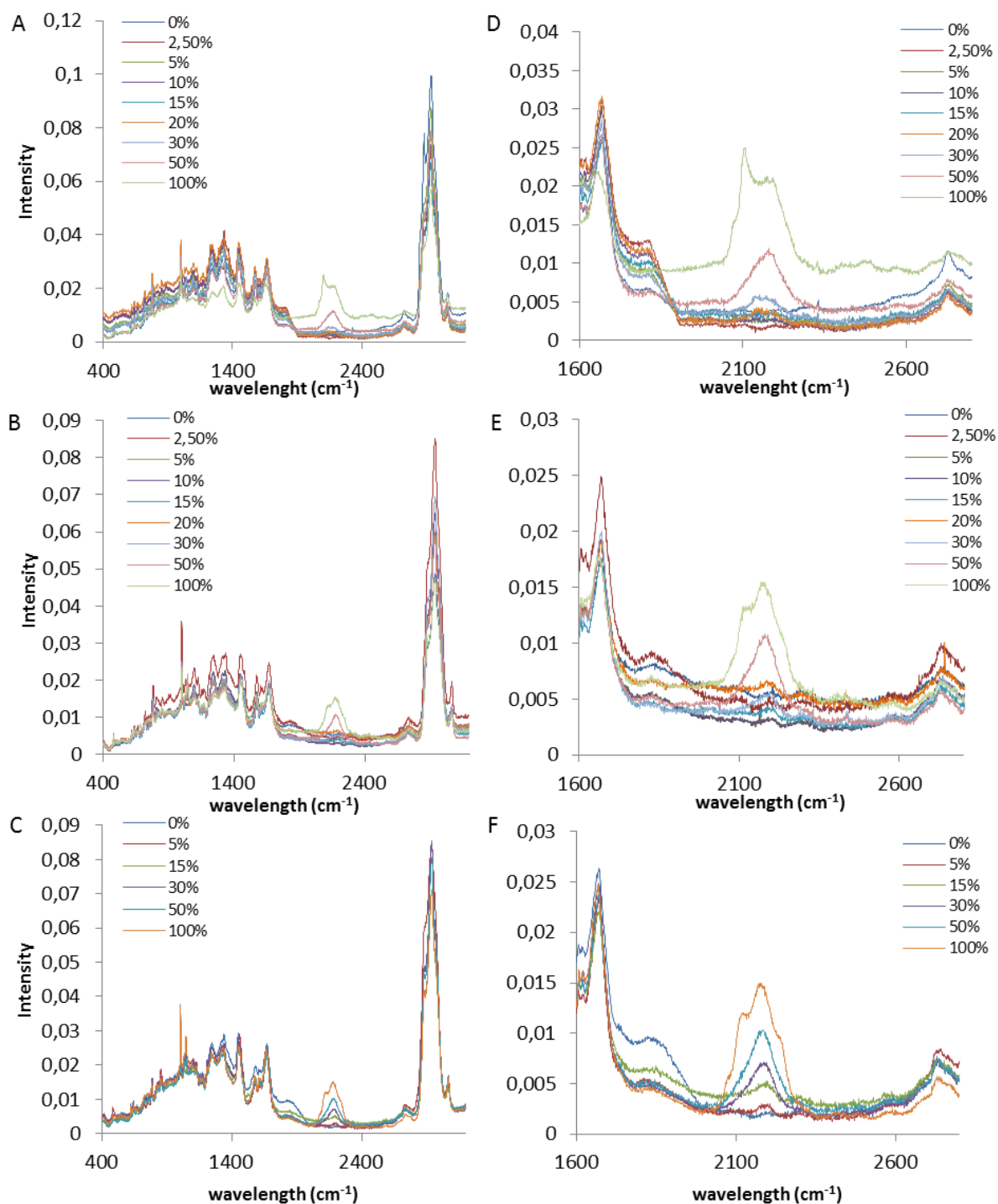
8. Supplementary

Figure S1: Raman spectra of (A) *E. coli*, **(B)** *B. subtilis* **and (C)** *B. thuringiensis.* **Mean spectra of 20-30 single cells grown in LB-medium containing increasing D$_2$O concentrations. The spectra were normalized and set to zero as described in Materials and Methods. (D-F) Detailed view of the CD peak area.**
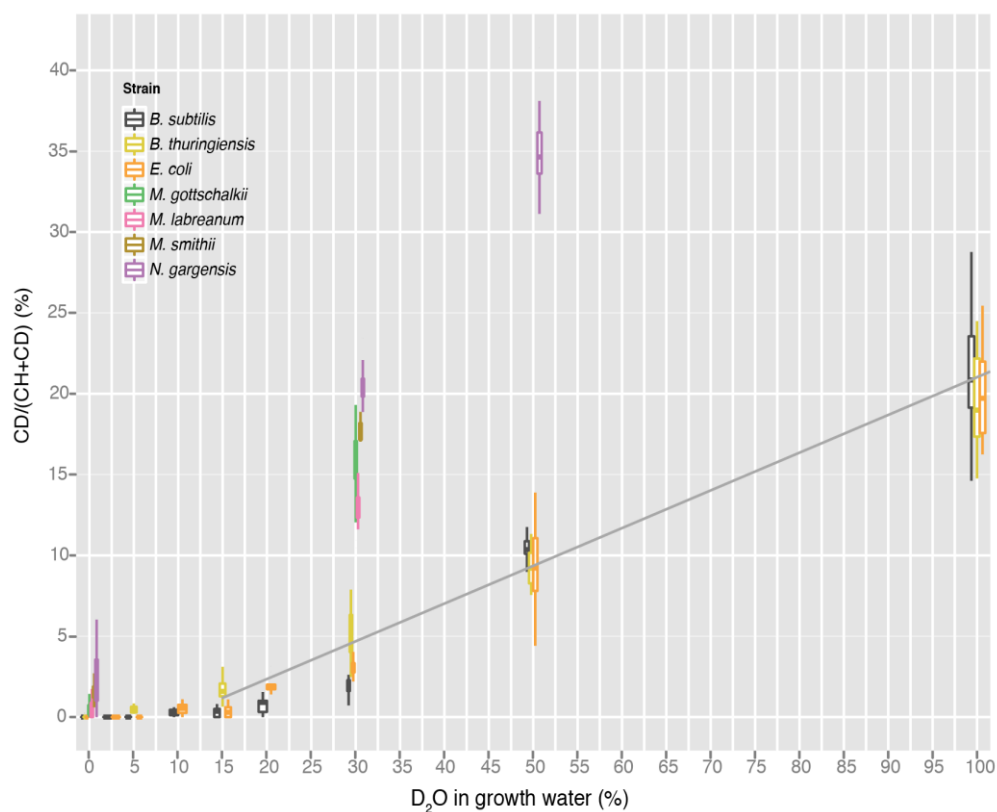
Figure S2: D incorporation in correlation to the growth water D$_2$O concentration. Various microbial strains (*Escherichia coli, Bacillus thuringiensis, Bacillus subtilis, Nitrososphaera gargensis, Methanobrevibacter gottschalkii, Methanobrevibacter smithii,* and *Methanocorpusculum labreanum*) were grown in medium containing varying amounts of heavy water. The %CD was calculated as described in Materials and Methods. Population quartiles are shown as boxplots. The detection limit (mean + 3s.d. of %CD in unlabeled cells) is below 1 for all tested bacteria, but slightly higher for the tested archaea (e.g. 3.75 for *M. smithii* and 7.88 for *N. gargensis*). The higher detection limit of the archaea is due to the small cell size and relatively high autofluorescence of these strains. The heterotrophic test strains were labeled relative to the concentration of D$_2$O in the growth medium (grey line, linear regression R^2 = 0.93). Graph adapted from (Berry et al., 2015)
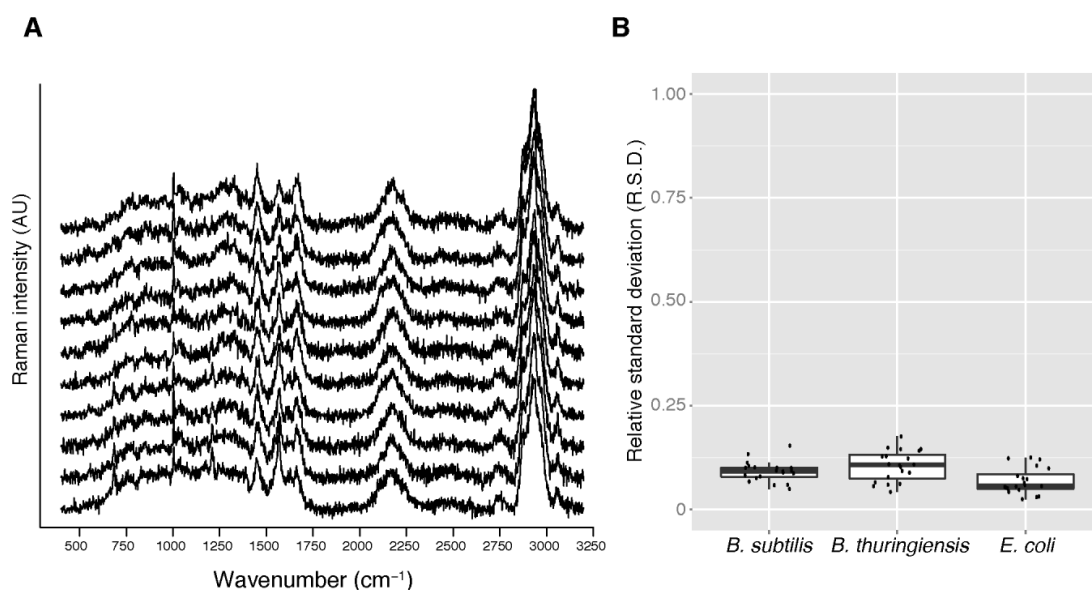
Figure S3: Reproducibility of %CD determined by repeated measurements of single cells. (A) Representative *B. subtilis* cell measured 10 times. The %CD over all spectra had a mean of 22.8 and a relative standard deviation (R.S.D. the standard deviation normalized to the mean) of 0.09. **(B)** Summary of the R.S.D. of *Escherichia coli*, *Bacillus thuringiensis*, and *Bacillus subtilis* cells grown in medium with 100% D_2O. Twenty cells of each strain were measured each ten times. Each point is the R.S.D. of a single cell and population quartiles are shown as boxplots. The mean R.S.D. over the three strains is 0.09. The Raman laser beam has an approximate focus size of 1 μm which is the size of a typical cell. In this regard different parts of the cell were measured to disclose any differences of the CD content within the cell. Graph adapted from (Berry et al., 2015)
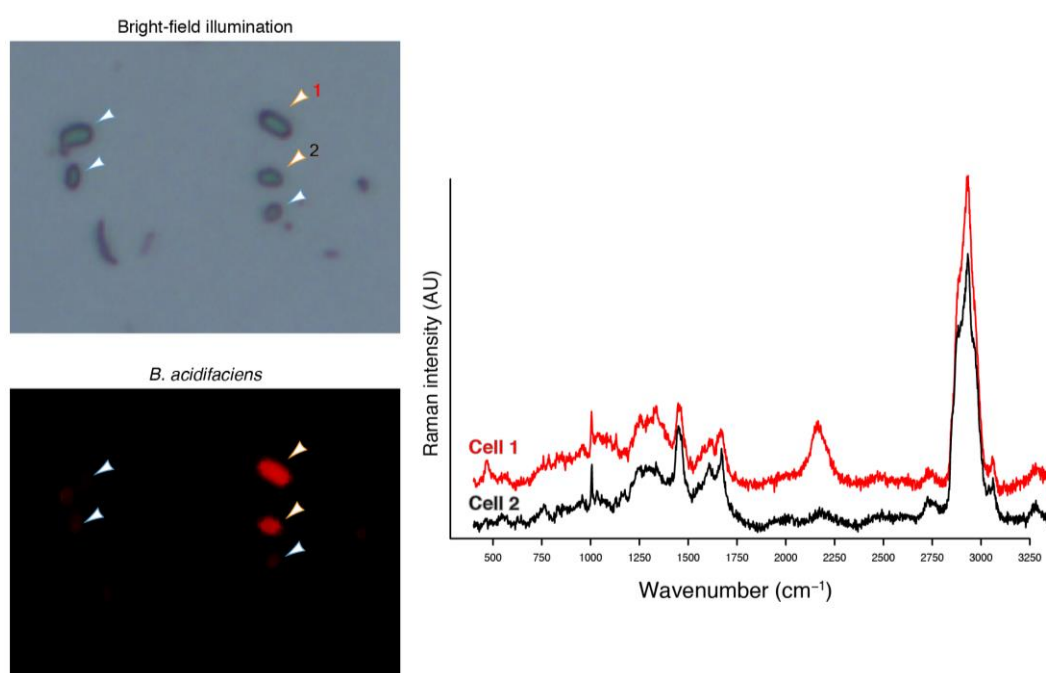

Figure S4: Combination of Raman microspectroscopy and FISH. Microscopic images (bright-field and epifluorescence) of the same field of view. *Bacteroides acidifaciens* cells from the mouse cecum incubation with glucose are labeled with a species specific FISH probe in red and indicated by arrows with yellow borders. Arrows with blue borders indicate other cells. The single cell Raman spectra of the stained cells show the presence of the CD peak (2040-2300 cm^{-1}) in one cell (red spectrum) and its absence or very low level in the second cell (black spectrum). This demonstrates that Raman-FISH can be used to visualize physiological intra species heterogeneity. Graph adapted from (Berry et al., 2015)
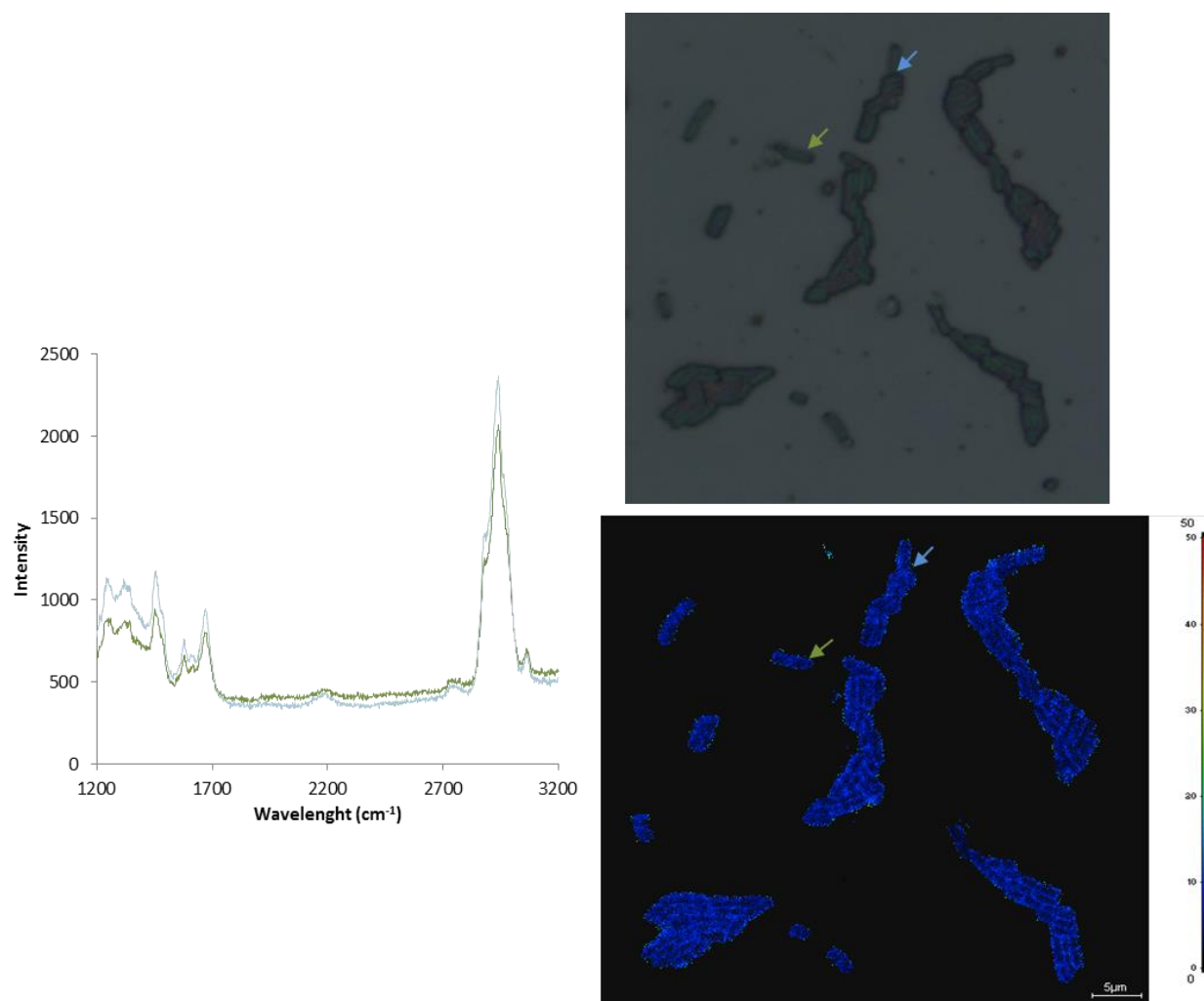
49

Figure S5: Isotope distribution (NanoSIMS) and Raman image of the same field of view. The Raman spectra displayed correspond to the cells marked by arrows in the pictures. The CD peak was slightly less prominent in the green denoted cell spectrum which is also represented in the corresponding region in the isotopic distribution picture with 4.20 at% D in contrast to 5.02 at% D in the blue denoted cell.

Table 1. The 16S rRNA-targeted probes used in this study for fluorescence in situ hybridization (FISH)

RDP II probe match[a]

Target	Name	Sequence (5'-3')	Formamide, %	Total hits	Major target taxa (coverage %, total hits in taxon)	Total nontarget hits	Major nontarget taxa (coverage %, total hits in taxon)	Source
All bacteria	EUB338 (S-D-Bact-0338-a-A-18) EUB338-II (S-*-BactP-0338-a-A-18) EUB338-III (S-*-BactV-0338-a-A-18) the three probes were applied as mixture	GCT GCC TCC CGT AGG AGT GCA GCC ACC CGT AGG TGT GCT GCC ACC CGT AGG TGT	35	1,948,215 12,640 24,385	Domain Bacteria (91.4%, 1,947,942) Order Planctomycetales (60.8%, 6,688) Phylum Verrucomicrobia (87.3%, 17,771)	273 5,952 6,614	- Unclassified bacteria (3.8%, 3,988) Family Anaerolineaceae (24.1%, 4,062)	1 2 2
Control probe complementary to EUB338	NON-EUB	ACT CCT ACG GGA GGC AGC	35	3	NA	3	-	3
B. acidifaciens	Baci731A_87 (S-*-BacA-87-a-A-24) Baci731B_87 (S-*-BacB-87-a-A-22)	GCG CCG GTC GCC ATC AAA AGT TTG G CCG GTC GCC ATC GGA AGT TTG	35	140 55	Genus Bacteroides Group-2 (89%, 124) Genus Bacteroides Group-1 (95%, 52)	2	-	6
Akkermansia spp	Akk1437 (S-G-Akk-1437-a-A-20)	CCT TGC GGT TGG CTT CAG AT	25	283	Genus Akkermansia (87.3%, 282)	1	-	4,5

1)   Amann R. I., Binder B. J., Olson R. J., Chisholm S. W., Devereux R. and Stahl D. A. (1990). Combination of 16S rRNA-targeted oligonucleotide probes with flow cytometry for analyzing mixed microbial populations. Appl. Environ. Microbiol. 56: 1919-1925.

2)   Daims H., Brühl A., Amann R., Schleifer K.-H. and Wagner M. (1999). The domain-specific probe EUB338 is insufficient for the detection of all Bacteria: Development and evaluation of a more comprehensive probe set. Syst. Appl. Microbiol. 22: 434-444.

3)   Wallner G., Amann R. and Beisker W. (1993). Optimizing fluorescent in situ hybridization with rRNA-targeted oligonucleotide probes for flow cytometric identification of microorganisms. Cytometry. 14: 136-143.

4)   Berry D, Schwab C, Milinovich G, Reichert J, Ben Mahfoudh K, Decker T, Engel M, Hai B, Hainzl E, Heider S, Kenner L, Müller M, Rauch I, Strobl B, Wagner M, Schleper C, Urich T, Loy A. (2012). Phylotype-level 16S rRNA analysis reveals new bacterial indicators of health state in acute murine colitis. ISME J. 6: 2091-106.

5)   Derrien M, Collado MC, Ben-Amor K, Salminen S, de Vos WM (2008). The Mucin Degrader Akkermansia muciniphila Is an Abundant Resident of the Human Intestinal Tract. Appl Environ Microbiol. 74(5): 1646–1648.

6)   Ramesmayer J., (2013). The painted gut: Establishing a comprehensive fluorescence *in situ* hybridization (FISH) probe set to illuminate abundant members of the mouse intestinal microbiota.

a) RDP (Ribosomal Database Project) II probe match was performed with database release 10, Update 32 (September 25, 2013) containing 2,765,278 bacterial and archaeal 16S rRNA sequences. The search for each probe was restricted to sequences of good quality with data in the respective probe-binding region. Coverage is the percentage of sequences within the RDP II target taxon that shows a full match to the probe sequence. The number of nontarget hits indicates the total number of sequences outside the respective RDP II target taxa that show a full match to the probe sequence.

9. Acknowledgments

This master thesis was performed at the Department of Microbiology and Ecosystem Science, Division of Microbial Ecology of the Vienna Ecology Centre (University of Vienna) and would have not been possible without the help of the following people.

I kindly want to thank:

- Michael Wagner for giving me the opportunity to do my master thesis and for giving me the opportunity to become a member of the Raman group.

- Dagmar Woebken and David Berry for their supervision and support throughout my thesis, and especially David without his statistical work this would have not been possible.

- Markus Schmid for helping me to master the Raman microspectroscopy and for always being there for questions and problems.

- Márton Palatinszky for always encouraging me and for critical reading my master thesis.

- Christoph Böhm for introducing me into the lab work during my Großpraktikum.

- All the other members of the Raman group for helpful discussions and support.

- Isabella Rauch and Buck Hanson for extracting the mouse gut community.

- Arno Schintlmeister for his patient introduction into NanoSIMS.

- Itzhak Mizrahi for providing the samples of methanogenic archaea.

- Jasmin, Michi, Kathi, Stephan, and all the other members of DOME for all the support, advice and fun. And also for not letting me forget to enjoy the sun in between.

In the end I have to thank my family for their support and for encouraging me always to do what I am interested in. And especially I want to thank Mario who was there for me the whole time and for sharing his life with me.

10. Curriculum Vitae

Personal data

Esther Mader BSc.

Date of birth	29.11.1986
Place of birth	Gerasdorf bei Wien
Nationality	Austria

Education

1993-1997	Volksschule Gerasdorf bei Wien
1997-2001	Hauptschule Gerasdorf bei Wien
2001-2006	BORG I Hegelgasse 12
2006-2009	study of history of arts, University of Vienna
since 2007	study of biology with focus on ecology, University of Vienna
since 2013	master thesis at the Division of Microbial Ecology, University of Vienna